Vertical walls and low reflection alternatives

Results of wave flume tests

M W McBride
N W H Allsop
P Besley
D Colombo
L Madurini

Report IT 417
April 1995

HR Wallingford

Address and Registered Office: HR Wallingford Ltd. Howbery Park, Wallingford, Oxon OX10 8BA
Tel: + 44 (0)1491 835381 Fax: + 44 (0)1491 832233

Contract

The work described in this report was funded by the Department of the Environment Construction Directorate (DoE) under research contract PECD 7/6/298, "The hydraulic design of harbour entrances" and by the Department of Transport. The DoE nominated officer for this contract was Mr P B Woodhead and HR Wallingford's nominated officer was Dr W R White, Research Director. The report is published on behalf of the DoE but any opinions expressed are not necessarily those of the funding department. The research described in this report was carried out in the Ports and Estuaries Group, managed by Dr J V Smallman, and the Coastal Structures Section, managed by Professor N W H Allsop, at HR Wallingford. The HR job number was DAS 0042.

Prepared by .... (name) Project Engineer .... (Job title)

Approved by J. V. Smallman .... Director ....

Date 20 May 1996

Summary

Vertical walls and low reflection alternatives
Results of wave flume tests

M W McBride
N W H Allsop
P Besley
D Colombo
L Madurini

Report IT 417
April 1995

Waves reflected from vertical breakwaters or other highly reflective structures forming port entrances can cause serious problems to vessel navigation. This often leads to port closures as vessels are unable or unwilling to enter or leave the port.

This report describes all aspects of a 2D physical model study. This study was initiated to examine the reflection and overtopping performance of various 'low reflection' structures under irregular wave attack. It is these types of structures which can be used in the modification or construction of port entrances to reduce wave reflections, and so improve conditions for vessel navigation.

Four main structures were tested consisting of a smooth vertical wall, single and double chamber wave screens and rock armour slopes. Various arrangements of these structures were tested to identify the optimum configurations.

The study found that the use of single and double chamber wave screens is effective in reducing wave reflections and overtopping. From the analysis of these results, an empirical formula was derived which can be used to describe the reflection performance of such structures, within practical engineering limits.

This report also describes a new technique to examine the effect of 'low reflection' structures on wave conditions. This was carried out through the analysis of local wave steepness. Previously a description of the reflection performance and overtopping of a structure was used in the assessment of the likely effect of wave reflections, and hence the relative changes in wave height, on vessel navigation. However, vessel navigation problems are not only related to wave height as the wave period is also significant in the creation of hazardous conditions. This new technique enables both relative changes in wave height and wave period to be considered, allowing a better assessment of the effect on vessel navigation to be made.

Notation

A_c	Armour crest freeboard, relative to SWL
a,A,b,B	Empirically derived coefficients
B_w	Width of structure or element, usually width of voided chamber or spacing between perforated and solid screens
B_w/L_s	Relative chamber depth
C_r	Reflection coefficient, defined H_{sr}/H_{si}
$C_r(f)$	Reflection coefficient function over frequency
C_t	Transmission coefficient, defined H_{st}/H_{si}
D_h	Hole diameter, in wave screen
D_{n50}	Nominal particle diameter defined $(M_{50}/\rho_{r/c})^{1/3}$
f	Wave frequency, inverse of wave period
h	Water depth
h_s	Water depth seaward of toe of structure
h_t	Toe depth
H_s	Significant wave height, average of highest one-third of all wave heights
H_{si}	Incident significant wave height
H_{so}	Offshore significant wave height
H_{sr}	Reflected significant wave height
H_{st}	Transmitted significant wave height
$H_s(x)$	Significant wave height at measurement point 'x' metres from structure
$H_{1/10}$	Wave height, average of highest one-tenth of all wave heights
Ir_m	Iribarren number = $\tan\alpha / s_m^{0.5}$
k_c, k_x, k_y	Coefficients in reflection prediction equation, equation (2)
L	Wave length
L_h	Wave length in the local water depth h
L_s	Wave length in the local water depth h_s
M_{50}	Median unit mass, generally of armour units
n_a	Porosity (by area) of screen, area of holes as a percentage of total screen area
$\bar{Q}$	Mean overtopping discharge per unit length of structure $m^3/s.m$
Q'	Goda's dimensionless discharge parameter = $\bar{Q}/(2gH_{so}^3)^{0.5}$
Q*	Owen's dimensionless discharge parameter = $\bar{Q} / (T_m\, g\, H_s)$
Q#	Franco's dimensionless discharge parameter = $\bar{Q}/(gH_s^3)^{0.5}$
Re	Reynolds number, usually defined in terms of nominal armour unit diameter, D_n, or screen thickness, t_s
R_c	Structure crest freeboard relative to SWL
R_c/H_s	Relative crest height
r^2	Regression coefficient
s_m	Mean wave steepness, defined $2\pi H_s/gT_m^2$ for deep water
s_p	Peak wave steepness, defined $2\pi H_s/gT_p^2$ for deep water
$s_m(x)$	Mean wave steepness at probe, x metres seaward of the structure
s_{mi}	Mean incident wave steepness
S_i	Incident spectral energy
S_r	Reflected spectral energy
T_m	Mean wave period

Notation Contd

T_p	Peak wave period (usually offshore)
t_s	Screen thickness
x	Distance of measurement point (wave probe) from structure
α (alpha)	Structure slope angle to the horizontal
β (beta)	Angle of wave attack, relative to the normal to structure
ξ	Surf similarity parameter, or Iribarren number, = $\tan \alpha / s^{0.5}$
ξ_m	Iribarren number = $\tan \alpha / s_m^{0.5}$
Δ	Fractional density of (eg) armour with respect to (sea) water
ρ	Mass density
ρ_r, ρ_c, ρ_w	Mass density of rock, concrete, or (sea) water

Contents

Page

Title page
Contract
Summary
Notation
Contents

1 **Introduction** . . . 1
1.1 Background . . . 1
1.2 Scope of work . . . 1
1.3 Outline of report . . . 2

2 **The physical model** . . . 2
2.1 Model construction . . . 2
2.1.1 Vertical wall . . . 2
2.1.2 Wave screens / perforated caissons . . . 2
2.1.3 Rock armour slopes . . . 3
2.2 Wave generation . . . 3
2.3 Data collection and analysis . . . 3
2.3.1 Water surface elevations . . . 3
2.3.2 Wave reflections . . . 3
2.3.3 Wave overtopping . . . 4
2.3.4 Wave pressures . . . 6

3 **Description of tests** . . . 6
3.1 Wave conditions and calibration . . . 6
3.2 Test methodology . . . 6

4 **Discussion of reflection results** . . . 7
4.1 Vertical walls . . . 7
4.2 Wave screens / perforated caissons . . . 7
4.3 Rock armour slopes . . . 9

5 **Discussion of overtopping results** . . . 11
5.1 Vertical wall . . . 11
5.1.1 Analysis using offshore wave heights . . . 11
5.1.2 Analysis using inshore wave heights . . . 11
5.1.3 Summary of results for vertical wall . . . 12
5.2 Wave screens / perforated caissons . . . 12
5.3 Rock armour slopes . . . 14

6 **Discussion of water surface conditions** . . . 14

7 **Scale effects** . . . 17

8 **Conclusions and Recommendations** . . . 17
8.1 Conclusions . . . 17
8.1.1 Reflection analysis . . . 17
8.1.2 Overtopping analysis . . . 18
8.1.3 Water surface conditions . . . 19
8.2 Recommendations . . . 19

9 **Acknowledgements** 19

10 **References** 20

Tables

Table 1 Wave conditions and wave screen spacings in terms of B_w/L_s
Table 2 Test programme
Table 3 Wave reflections from vertical wall, Test Series 1000
Table 4 Coefficients in Equation (2) for tested screen configurations
Table 5 Results of water surface analysis

Figures

Figure 1 Model configuration with bathymetry
Figure 2 Model caisson with double chamber wave screen at B_w = 0.575m
Figure 3 Perforated wave screen, n_a = 20%
Figure 4 Vertical wall with rock armour slope
Figure 5 Comparison of reflection analysis methods
Figure 6 Overtopping of simple vertical walls, comparison of Herbert (1993) and Goda (1985)
Figure 7 Influence of relative crest height on reflections
Figure 8 Reflections from single chamber with hole diameters = screen thickness, n_a=20%, curve 1, eqn (6a)
Figure 9 Reflections from single chamber with hole diameters = 2 x screen thickness, n_a=20%, curve 2, eqn (6b)
Figure 10 Influence of part-depth floors, water level at +1.61m
Figure 11 Reflections from double chamber with hole diameters = 2 x screen thickness, n_a=20%, curve 4
Figure 12 Influence of part-depth floors, water level at +1.43m
Figure 13 Reflections from double chamber with hole diameters = screen thickness, n_a=20%, curve 3
Figure 14 Reflection performance of smooth and armoured slopes, after Allsop (1990)
Figure 15 Reflections from armoured slopes in front of vertical wall
Figure 16 Piled quay over armoured slope on part-depth caisson
Figure 17 Reflections from alternative coal berth quays
Figure 18 Comparison between Herbert's results and Series 1000
Figure 19 Simple vertical walls, Series 1000, Owen's equation
Figure 20 Simple vertical walls, Series 1000, Franco's equation
Figure 21 Franco's equation using offshore and inshore wave heights
Figure 22 De Waal's data with Owen's equation, A=0.002 and B=26.76
Figure 23 De Waal's data with Franco's equation, a=0.03 and b= -2.05

Contents continued

Figure 24	Single and double chamber wave screen structures, Series 2100, 3100 and 3200
Figure 25	Wave screen structures, large holes, Series 4200 and 4100
Figure 26	Wave screen structures, B_w=0.40m, Series 2200 and 3300
Figure 27	Caisson chambers with raised floors, Series 500 and 6000
Figure 28	Overtopping of vertical wall with armoured slopes
Figure 29	Water surface conditions - Vertical wall
Figure 30	Water surface conditions - Single chamber wave screen
Figure 31	Water surface conditions - Double chamber wave screen
Figure 32	Water surface conditions - Rock armoured slope
Figure 33	Analysis of scale effects for wave screens tested with small wave heights

1 Introduction

1.1 Background

Previous work by McBride et al (1993) discussed problems arising from wave reflections in harbours. It was found that these problems were caused by the use of vertical or near vertically faced structures to form harbour boundaries. This work also reviewed various types of 'low reflection' structures for which some performance data were known. That review was followed by studies using physical and numerical models of harbour entrances which is reported by McBride et al (1994 and 1995). Those studies suggested that wave disturbance problems in many harbour entrances would be substantially reduced if wave reflections from the primary harbour structures were kept below 40%. The reflection performance of most vertical breakwaters and harbour walls falls in the range of 90 to 100%, so substantial reduction in reflections may be required.

This report describes tests to quantify the reflection and overtopping performance of vertical breakwaters and 'low reflection alternatives', and discusses the analysis of the reflections and an initial analysis of the overtopping measurements. The work described in this report has been used in the preparation of guidelines for the hydraulic design of harbour entrances, McBride et al (1996).

1.2 Scope of work

The simplest structure considered in these flume tests was a smooth vertical wall. The wave height, wave steepness, and local water level were all varied. Low reflection structures were formed by mounting perforated screens in front of the wall, or by adding an armoured rubble slope in front of the vertical wall. The former configuration simulated a range of perforated face caissons, some of which had raised floors within the chambers. The latter configuration simulated the addition of armour in front of an existing wall, or the substitution of an armoured slope, perhaps beneath a piled quay. The sections which were tested are summarised below:

Test Series	Structure tested
1000	Vertical structure only
2000	Vertical wall and single wave screen
3000	Vertical wall and double wave screen
4000	Vertical wall and single / double wave screen
5000	Double wave screen, chamber floors at 30% depths
6000	Double wave screen, chamber floors at 30 and 50% depths
7000	Rock armour slope 1:1.5, 2 stone berm width at +1.71m
8000	Rock armour slope 1:1.5, 2 stone berm width at +1.61m

1.3 Outline of report

This report details all aspects of these flume tests. Chapter 2 provides a description of the physical model construction and layout, with the details of the wave conditions and test methodology given in Chapter 3. The discussion of the results is divided into three chapters (4, 5 and 6), in order that the three main areas for discussion, wave reflections, overtopping and wave conditions with regard to navigation, are considered independently. Cross referencing between these chapters has been used where it has been considered appropriate. Chapter 7 discusses the potential scale effects and Chapter 8 summarises the conclusions of this work.

2 The physical model

2.1 Model construction

The 2-dimensional tests were conducted in the Deep Random Wave Flume at Wallingford. This flume is 52m long, and operates with water depths at the paddle between 0.8m and 1.75m. The flume is configured to reduce re-reflection of un-wanted wave energy from the test section by the use of absorbing side channels, either side of, and separated from the central channel by perforated dividing walls.

The bathymetry in front of the structure was formed in cement mortar to a uniform slope with a gradient of 1:50, as shown in Figure 1. The bed level at the position of the structure was +1.00m relative to the wave flume floor. In front of the test structure, a number of channels were moulded into the sea bed, parallel to, and seaward of the vertical wall. These channels were used to secure the base of each perforated screen at given spacings from the vertical wall. Example spacings between two perforated screens placed in front of the caisson are shown in Figure 2, and the full range of screen spacings are summarised in Table 1.

2.1.1 Vertical wall

The vertical wall was formed using a caisson. The main caisson section was formed as a hollow box in marine plywood, with a crest level at +1.8025m, ie. the crest was 0.8025m above the toe. The use of a hollow box enabled overtopping collection/measurement equipment to be installed inside the box, reducing the need for any external collection or measurement devices. The seaward side of the box, which formed the vertical wall, was faced with a stainless steel plate to aid the installation of pressure measurement equipment, which was used in subsequent testing to examine wave impact and up-lift pressures. The caisson section was only installed in the flume after wave calibrations, so those wave measurements were not contaminated by any reflected waves. The caisson section was used alone for those tests on the vertical wall.

2.1.2 Wave screens / perforated caissons

Two pairs of wave screens were constructed from marine plywood with a thickness of 25mm. These were perforated to an area porosity of n_a = 20%. The first pair of screens were perforated by circular holes with a diameter of 25mm, equal to the screen thickness. The holes in the second pair of screens were formed with a diameter of 50mm, twice the screen thickness, as shown in Figure 3. Identical pairs of screens were constructed to enable testing of single and double chamber wave screens. When installed in their respective channels in the sea bed all screens had a crest level of 0.8025m above the toe, +1.8025m relative to flume floor. The screens were used to form voided chambers of overall width, B_w, of 0.575m or 0.400m. During tests on double wave screens, the chamber was split into two chambers by a second perforated screen at half the spacing, as shown in Figure 2.

2.1.3 Rock armour slopes

A common modification to simple vertical walls in harbours is the construction of a rubble or rock armour slope against the wall. The rough and porous armour layers dissipate wave energy, thus reducing wave reflections, and also, in many cases, overtopping. However, for some combinations of water level, armour crest level, and wave conditions, the slope can lead to an increase in overtopping. Hence, rock armour slopes were included to explore the potential of adding such slopes in front of an existing vertical wall. Previous studies by Allsop & Hettiarachichi (1988) and Allsop & Channel (1989), reported by Allsop (1990), provide details of reflection performance for simple armoured slopes without wave walls or other reflective elements. Some indication of the potential influence of a vertical wall behind the slope are given by ad hoc studies of armoured slopes beneath a piled quay, reported by Allsop (1990). Therefore, two rock armour slopes were tested to examine the effects of changing the armour crest level, and hence the relative armour freeboard. Both armour slopes were placed at 1:1.5 with armour with a nominal particle diameter, D_{n50}, of 0.074mm, and a crest berm width of $2D_{n50}$. The two armour berm levels, which were tested, were +1.61m, see Figure 4, and +1.71m, with the caisson crest at +1.8025m. Tests on this structure in series 7000 and 8000 used water levels of +1.61m and +1.43m.

2.2 Wave generation

Waves were generated by a sliding wedge paddle, driven by double acting hydraulic rams. The paddle is computer controlled using software developed at HR Wallingford. This software enables either regular or random waves to be produced. The random wave signals are generated to match any wave spectrum that can be specified at 16 equal frequency ordinates. JONSWAP spectra were generated for all of the tests. The nominal wave heights in Table 1 were generated and measured in the deep water section of the flume.

2.3 Data collection and analysis

2.3.1 Water surface elevations

Measurements of water surface elevations were made using 8 twin wire wave probes, located along the approach to the vertical wall. Spectral and statistical analyses allowed the significant, 0.1%, and other extreme values of the wave height distribution to be determined at each monitored position, together with the mean wave periods. The measurements from three of these probes were used to determine the reflection coefficient, described in Section 2.3.2. Analysis of total water surface excursions and periods from these and other probes enabled the determination of the likely effect on vessel navigation, as described in Chapter 6.

2.3.2 Wave reflections

Incident and reflected wave conditions were measured using three of the twin wire wave probes, located approximately 2 wave lengths seaward of the structure. Each test was run for 1000 waves and output from the 3 probe array was analysed to give the reflection coefficient function, $C_r(f)$, over a range of wave periods, equivalent to 0.5 to $2.0T_p$, using the method of Gilbert

& Thompson (1978) based on the approach of Kajima (1969). The overall reflection coefficient, C_r, was determined by summing energies for each test condition.

Gilbert & Thompson's method for the reflection coefficient, the 'HR method', has recently been checked against the method of Davidson (1992) at Plymouth University, referred to as the 'Plymouth method'. Davidson argues that the main difference between the methods lies with the manner in which they reject data which is contaminated with singularities. Both methods were used to analyse waves reflected from armoured slopes in the same wave flume at Wallingford. The results of this comparison are summarised in the simple comparison shown in Figure 5. These show very close agreement over the range tested. Two alternative regression lines have been fitted, namely $y = 0.96x$ and $y = 1.04x - 0.05$. Both lines gave a regression coefficient, r^2, of 0.97. This simple comparison suggests that the error in the determination of C_r from either method is likely to be less than about 5%.

2.3.3 Wave overtopping

During most of these tests, the number of waves overtopping the structure, the wave by wave overtopping volumes, and the mean overtopping discharges, were each determined. The number of waves overtopping the structure were counted using four overtopping probes spaced across the width of the flume. The overtopping discharge was determined from overtopping volumes measured using a weighing mechanism located inside the caisson which formed the vertical wall. A 100mm wide chute directed overtopping water into the tank. The sensitivity of the weighing mechanism allowed the measurement of wave by wave overtopping discharges. The mean overtopping discharge was calculated at the end of each test. When a high mean overtopping discharge was expected during a test, the weighing cell was removed and a large reservoir was used to collect the water. The water was then pumped into calibrated volumetric cylinders.

Overtopping of vertical walls

The main method to predict wave overtopping of vertical walls is based on a graphical method developed by Goda (1985). For a given approach bed slope, m, and offshore sea steepness, $s_{om} = 2\pi H_{so}/gT_m^2$, a dimensionless discharge, $Q' = \bar{Q}/(2gH_{so}^3)^{0.5}$, is plotted against h_s/H_{so}, where H_{so} is the offshore significant wave height, h_s is the water depth at the toe of the structure and $\bar{Q}$ is the mean overtopping discharge in m^3/s per metre run of sea wall.

Recent tests by Herbert (1993) have confirmed and extended this approach for steeper waves and shallower bed slopes. These graphs are plotted as iso-lines of R_c/H_{so}, for example a comparison of Herbert's results with Goda is shown in Figure 6. Dimensionless overtopping discharges, Q', rise to maxima around h_s/H_{so} = 1.2 to 1.7, which correspond approximately to the relative depth for the maximum inshore significant wave height. Above h_s/H_{so} = 1.2 to 1.7, the dimensionless discharge again reduces, corresponding to the region of depth-limited, and therefore, broken waves. It is important to note that Goda's method relies on the offshore wave height, H_{so}, the offshore wave steepness, s_{mo}, and the estimation of a simple sea bed slope (m = 1:10, 30 or 100). The inshore wave height is not used in this method, but is implied from the offshore wave height, period, sea bed slope, and the water depth five wave lengths offshore.

The main weakness of these methods is that the influence of the bathymetry can only be accounted for by choosing the nearest simple bed slope, m, and interpolating between graphs for given wave steepness, s_{mo} = 0.017, 0.036 and 0.045 without data for steeper waves. It must also be noted that these are manual graphical methods and therefore they can not be readily incorporated into other calculation method, eg. risk or joint probability analysis.

Further work by Franco (1993) suggests that there may be a simple relationship between an alternative dimensionless discharge, Q#, and R_c/H_s for vertical walls or perforated vertical walls, with and without crest detail, where $Q\# = \bar{Q}/(gH_s^3)^{0.5}$. The work was based on physical model test results with wave steepness in the range $0.018 < s_m < 0.038$. Franco (1993) showed that overtopping of a vertical wall can be described by a simple empirical formula:

$$Q\# = a \exp (b\ R_c/H_{so}) \qquad \text{where } a = 0.2 \text{ and } b = -4.29 \qquad (1)$$

<u>Overtopping of sloping walls</u>

Studies carried out in the UK on a wide range of sloping walls in the late 1970s have shown that it is useful to express the discharge, $\bar{Q}$, as a dimensionless parameter Q*, and the crest freeboard as R*, where:

$$Q^* = \bar{Q} / (T_m\ g\ H_s\ ) \qquad (2a)$$

$$R^* = R_c / (T_m\ (g\ H_s)^{0.5}) \qquad (2b)$$

R_c is the crest freeboard above still water level, H_s and T_m are the significant wave height and mean wave period respectively. These parameters were used by Owen (1980) to suggest a simple empirical relationship between Q* and R* for simple and bermed slopes:

$$Q^* = A \exp (-BR^* / r) \qquad (3)$$

Values of the empirical coefficients A and B depend on the slope angle. Values of the relative roughness coefficient, r, which are less than 1.0 imply overtopping levels below those of the equivalent smooth slope. Owen suggests values of the relative roughness coefficient for different armour types and these are summarised below, based on run-up experiments in the Netherlands:

Armour Type	Roughness value, r
Smooth, impermeable	1.00
Rough concrete	0.85
Pitched stone in mortar	0.75 - 0.80
Two layers of rubble	0.50 - 0.60

The methods developed for simple sloping seawalls have been extended by Owen & Steele (1991) to include the influence of wave return walls, and by Besley et al (1993) to include the effects of armoured slopes, and crest berms. Discharge reduction factors take account of the influence on the overtopping discharge of a berm or wave wall.

For armoured slopes, values of the run-up reduction factor r have been derived directly by analysing the overtopping of various armoured slopes, described by Allsop et al (1994b). Alternatively, new values of A and B can be derived for specific structures, using $r = 1$.

2.3.4 Wave pressures

Measurements of wave pressures on the front face of the caissons, the underside, and within the seaward toe of the rubble mound, were made but are not discussed in this report. These results are reported separately by McKenna et al (1994).

3 Description of tests

3.1 Wave conditions and calibration

The wave conditions used for testing are summarised in Table 1. This table also shows the spacings for the wave screen elements in terms of the relative wave length B_w/L_s for each wave condition, where B_w is the total chamber depth, and L_s is the mean period wave length calculated for the water depth at the structure, h_s. The primary spacings of B_w = 0.575m and 0.400m allowed the tests to cover the range $0.1 < B_w/L_s < 0.25$. The wide range of water depths and wave conditions ensured that the waves at the structure covered the full range from non-breaking waves, breaking waves, and depth-limited waves. The sea steepness, s_m, investigated covered the range of 0.02 to 0.06.

Wave conditions at a position equivalent to the breakwater were measured during calibration tests, before construction of the model breakwater structure. Short sequences of waves were generated during calibration and were determined using spectral analysis. Once the nominal wave condition had been achieved, more comprehensive measurements were then made using longer sequence lengths, analysed using statistical methods. This ensured that extreme waves were reproduced correctly, and that the statistical distribution of wave heights was recorded. Statistical analysis allowed the significant, 0.1%, and other extreme values of the wave height distribution to be determined at each wave probe position, together with the mean wave periods. These long wave sequences were used during testing to ensure that extreme waves were correctly represented.

3.2 Test methodology

The test programme is summarised in Table 2 which outlines the 137 tests conducted. All wave conditions presented in Table 1 were used for the vertical wall alone, and for the single chamber wave screen with a spacing of B_w = 0.575m. The combinations of wave conditions and water levels used for the subsequent tests were reduced based on analysis of the reflection and overtopping results from the initial tests. This enabled the test programme to be kept to a manageable size and to concentrate the analysis on comparable sets of test conditions.

Test series 1000 and 2000 addressed the vertical wall and a single chamber wave screen with two spacings. Overtopping at the highest water level, +1.71m was extremely high, and was judged to be unrepresentative of the degree of overtopping usually encountered in European harbours. Therefore no further tests were carried out at this water level.

An initial analysis of the results of Test Series 2000 suggested that the screen spacing of B_w = 0.575m was the optimum for the particular range of wave conditions used in these tests. This spacing was therefore used in Test Series 3000 to 6000 which involved modifications to the chambers and the screens, such as variations of the hole diameter in the porous screens, and the depth within the chambers. The last two test series, 7000 and 8000 explored the effect of rock armoured slopes placed against the vertical wall. Two crest levels were tested at two water levels, and the results provided information on the influence of the relative crest freeboard.

4 *Discussion of reflection results*

4.1 Vertical walls

The results of the reflection measurements in front of the plain vertical wall, Test Series 1000, are summarised in Table 3. In most instances C_r falls between 0.85 and 0.90, with relatively little influence of incident wave height or period. The water level, and crest freeboard were however of more influence, as summarised in Figure 7.

In general the larger and steeper waves lead to a slight reduction of reflections, due to higher levels of energy dissipation caused by wave breaking. However, an increase in the water level also lead to a reduction of reflections, but this was primarily due to the increased overtopping resulting from the lower structure freeboard, R_c. This is illustrated in Figure 7 where it can be seen that values of C_r are reduced at lower values of R_c/H_s. A simple prediction method was created through the use of regression analysis on the upper and lower regions of this data. This enabled an upper bound and a simple equation to be applied to these results as follows:

$$C_r = 0.79 + 0.11\ R_c/H_s \qquad \text{for } R_c/H_s < 1.0 \qquad (4a)$$
$$C_r = 0.90 \qquad \text{for } R_c/H_s > 1.0 \qquad (4b)$$

4.2 Wave screens / perforated caissons

Analysis of previous test results and of numerical model predictions by Allsop & McBride (1993) has shown that the most useful way of presenting the reflection performance of perforated wave screens is by plotting the reflection coefficient C_r against the relative screen spacing to wave length ratio, B_w/L_s. Results for Test Series 2000 are presented in this way in Figure 8. Results from previous studies by Allsop & Steele (1990) and Allsop & Beresford (1993) using a single slatted wave screen in front of an impermeable screen, for a harbour at Cardiff, have also been presented. Only comparable tests from this study were used, ie. those where the screen porosity was 20%, as the study covered a wide range of screen porosities. The results of tests with other screen porosities were discussed by Allsop & McBride (1993). Inclusion of the Cardiff results enabled the range of data to be extended beyond the maximum relative spacing of the most recent studies, ie. $B_w/L_s < 0.27$.

The results follow the general trends identified previously by Allsop & McBride (1993), ie. the minimum value of C_r is achieved when the porous screen is a little less than a quarter of a wave length from the solid wall, $B_w/L_s \approx 0.20$ to 0.25. The previous work demonstrated that initial estimates of reflection performance can be achieved using numerical models such as 'BARRIER2' by Bennett et al (1992). However, it is clear that such models cannot describe the influence of many of the detailed modifications studied here, and that simple empirical methods may be more appropriate in some circumstances.

These data have therefore been described by fitting a new empirical curve, given by:

$$C_r = \sin \{ k_c [(B_w/L_s) - k_x]^2 \} + k_y \qquad (5)$$

where k_c, k_x and k_y are coefficients determined from the data and:

- k_c determines the shape of the curve; low values (600) result in a shallow 'u' shaped curve, and high values (900) result in more steep 'v' shaped curves;
- k_x specifies the value of B_w/L_s which corresponds with the lowest point of the lowest value of C_r;
- k_y gives the lowest value of C_r.

The use of the test results allows values of these coefficients to be established for each configuration. Curve 1, shown in Figure 8, describes the results for a single chamber wave screen, with a porosity n_s = 20% and a hole diameter equal to the screen thickness:

$$C_r = \sin \{ 910 [(B_w/L_s) - 0.225]^2 \} + 0.28 \qquad (6a)$$

This equation is valid $0.05 < B_w/L_s < 0.32$. The use of equation (6a) outside this range is not supported by the results considered here, although its use for $0 < B_w/L_s < 0.05$ will probably give reasonable results. There is, however, seldom need for details of reflection performance outside of these limits as such structures will be uneconomic, or ineffective.

The modelling of the other structural variations enables values of the coefficients in equation (5) to be established for different structural configurations. The results, shown in Figure 9, for screens with larger diameter holes, ie. twice the screen thickness, show that the lowest value of C_r is increased, and the curve is slightly widened. Curve 2 can be described by the following version of equation (5):

$$C_r = \sin \{ 780 [(B_w/L_s) - 0.223]^2 \} + 0.315 \qquad (6b)$$

Curve 2, equation (6b), is shown as the solid line in Figure 9, where it may be compared with Curve 1, equation (6a), shown with crosses. The differences between these curves are relatively small. The other modifications tested have also been analysed to produce similar curves, and coefficients for equation (5) have been derived and are summarised in Table 4.

The effect of using double screens is shown in Figure 11 by comparing Curve 1 for a single chamber (shown as crosses) with Curve 3 for the double chambers (shown as the solid line). These show slightly lower reflections with a double chamber for $B_w/L_s > 0.2$, but rather higher reflections for $B_w/L_s < 0.2$. The use of the double screen increases the structure cost without significant benefit in reducing value of C_r, or increasing the range of B_w/L_s over which reflections are low. The lowest coefficient for the single screen, $C_r = 0.28$, occurs at $B_w/L_s = 0.225$, compared to $C_r = 0.265$ for the double screen at $B_w/L_s = 0.25$. The improved reflections given by the double screen for $B_w/L_s > 0.20$ are of relatively little benefit as the designers main requirement is to minimise the structure width B_w, and hence cost. However, this effect is less marked in comparing single and double screens with holes of a diameter equal to twice the screen thickness, Figures 9 and 11.

The reflection performance of voided caissons with perforations over the full depth of the structure are relatively insensitive to changes in water level. The last modifications to the caisson structures, where the voided chambers were filled to depths of 30% or 50% of the structure height, were rather more sensitive to changes in water level, as shown in figures 10 and 12.

In Test Series 5000 and 6000, reflections were measured for double chambers with the base of the chambers filled to depths of 30% or 50% of the chamber height. The base of the chambers were filled with blocks and rubble, and the holes in the front screen were blocked. For 30% restriction, the chamber was filled to +1.24m, and for 50% to +1.40m. In Series 5000, both chambers were filled to 30%, but in Series 6000, the floor in the rear chamber was raised by filling to 50%, giving a stepped arrangement. Each structure was tested with water levels of +1.43m or +1.61m. In each instance, the restriction in the volume of active voids of the chambers increased the reflection coefficient, with the most obvious effect occurring at the lower water level. The results of tests in Series 5000 are shown in Figure 12, with a comparison of results for the full depth chambers. The influence of the restrictions are quite significant, leading to an increase in reflections from C_r = 30% to 40% to C_r = 50% to 60%.

At the higher water level, +1.61m, the effect of this change, shown in Figure 13, is less marked, but still of significance. For the same wave heights and steepness, values of B_w/L_s change due to the influence of water depth on wave length. These reductions of B_w/L_s themselves might be expected to give slightly higher values of C_r. The larger area of open screen at the greater water depth gives lower reflections for the part-depth chambers, but C_r is still greater than for the full-depth chambers.

It must be noted that the work described in this section relates to simple, vertical structures. Hence, it may be the case that other structures, such as caissons constructed on rock mounds, may give different results due, in part, to the influence of the mound on the waves.

4.3 Rock armour slopes

Reflections from sloping structures are less severe than from vertical walls. The reflection characteristics of armoured and smooth slopes depend on wave breaking on the slope, and are related to the surf parameter or Iribarren number, ξ_m or Ir_m, defined $\xi_m = Ir_m = \tan\alpha/s_m^{0.5}$; where $s_m = 2\pi H_s/gT_m^2$. Reflections from smooth or armoured slopes may be described by a simple formula derived by Seelig (1983):

$$C_r = a\,\xi_m^2 / (b + \xi_m^2) \qquad (7)$$

This equation was later adapted by Allsop (1990) for random waves. Tests by Allsop & Channel (1989) derived coefficients a and b for smooth and armoured slopes, with wave conditions in the ranges of $0.004 < s_m < 0.052$, and $0.6 < H_s/\Delta D_{n50} < 1.9$. Results, shown in Figure 14 for smooth and armoured slopes, are described by equations (8a) and (8b) respectively:

$$C_r = 0.96\,\xi_m^2 / (4.8 + \xi_m^2) \qquad (8a)$$

$$C_r = 0.64\,\xi_m^2 / (8.85 + \xi_m^2) \qquad (8b)$$

The use of equation (8b) for rock armoured slopes is supported by recent analysis by Davidson et al (1994), who checked predictions using the coefficients derived by Allsop (1990), against field measurements from a rock armoured breakwater with good agreement.

Results from Test Series 7000 and 8000 are summarised in Figure 15 for the different armour crest levels. In each instance, the armour freeboard above the water level, A_c, is non-dimensionalised by the armour size, D_{n50}. Values of A_c/D_{n50} varied from zero, where nearly all waves hit the vertical wall, to 3.8, where the vertical wall had relatively little influence on the reflections. At intermediate armour levels, A_c/D_{n50} = 2.4 and 1.35, the reflections are close to those of the armour slope, but some influence of the armour slope and crest berm is evident in reflections below those predicted by equation (8b).

Armoured slopes are often used within harbours beneath piled decks or platforms. Reflections from this type of structure are generally close to those predicted for the armoured slope alone. However, some details of the structure may significantly modify its hydraulic performance, illustrated by the following example from Allsop (1990).

An unusual structure was considered for a major coal handling quay. The harbour design required low levels of wave reflections from the quays, but was also in a region subject to earthquakes under which conventional piled relieving platforms might be unstable. The two alternative structures which were tested in the design study were a simple armoured slope of 1:1.75 under a piled deck, and a composite structure with armoured slope on a part-depth caisson.

The composite structure, shown in Figure 16, incorporates two important differences when compared with the simple armoured slope. The lower face of the structure is vertical, which might be expected to increase reflections, and the crest level of the armoured slope is relatively low, hence, larger waves may reach the vertical step at the rear of the slope formed by the rear deck beam, again tending to increase reflections. The reflections from this structure are compared with the simple prediction curve for armoured slopes, equation (8b), in Figure 17.

Section A, representing the armoured slope of 1:2.5 over the part depth caisson, as shown in Figure 16, had an armour crest berm on which larger waves could be absorbed. These gave reflections close to, but below those predicted by equation (8b). The reduced reflections arose due to the interference between the wave component reflected by the vertical part, and that reflected by the slope. The structural variation A2 had a crest detail in which more wave action reached the crest beam, which lead to an increase in reflections. The alternative section, B, which used a full-depth slope of 1:1.75, but included the crest detail of A2, resulted in reflections greater than the predictions.

This example demonstrates that, whilst the reflection performance of simple slopes is relatively easy to predict, reflections from composite structures may be significantly influenced by relative water levels, particularly where these water levels approach the level of the armour crest, or of other structural elements.

5 Discussion of overtopping results

The methods described in Section 2.3.3 have each been used to analyse the overtopping measurements made during this test programme. For the vertical wall only test case, overtopping discharges were compared with predictions made using Goda's curves. The methods of Owen (1980) and Franco (1993) were used to analyse all of the data sets described below. The overtopping measured during tests with the rubble slopes in front of the vertical wall have been compared with the prediction method of Owen & Steele (1991).

5.1 Vertical wall

5.1.1 Analysis using offshore wave heights

A series of general prediction lines, which was derived by Herbert (1993) for random waves, is plotted in Figure 6, with those derived by Goda (1985) for a vertical wall on a 1:30 slope, with an incident wave steepness of s_{mo} = 0.036.

The data from the present set of tests, Series 1000, for an approach slope with m = 1:50 have been combined with Herbert's data for s_{mo} = 0.06, and a slope of m = 1:30, as shown in Figure 18. Offshore wave conditions were measured and H_{so} and T_{mo} were used in the following analysis. No comparison with Goda is possible as the wave steepness exceeds s_{mo} = 0.045.

The results shows good agreement between the two studies, despite the very different relative depths due to the difference in model scales. Water depths and wave heights used in the present study are approximately 3 times larger than those used by Herbert (1993). Again, the use of this method shares the disadvantages identified in Section 2.3.3, and requires careful interpolation for the different values of R_c/H_{so}.

5.1.2 Analysis using inshore wave heights

The overtopping performance of a wall in relatively shallow water depends on the inshore wave height, period and shape. Using the offshore wave conditions only, as in the Goda method, confuses the analysis as it looses information on the form of the waves inshore. The form of the inshore waves depends on the water depth, foreshore slope, as well as the wave height and period. In this study, the inshore wave conditions were measured at the toe of the structure during wave calibration. These wave conditions have been used in the following analysis of the data from these tests.

The simplest analysis method is offered by plotting Owen's dimensionless discharge and freeboard parameters Q* and R* using exponential or logarithmic axes. These are shown in Figure 19 using the inshore wave height H_{si} from the calibrations. The data shows a good relationship between lnQ* and R*, so a simple regression line has been fitted, giving A = 0.002 and B = 26.76 in equation (3). This regression line is used in later figures to compare the overtopping performance of the vertical walls with that of the alternative structures.

The tests described by Franco (1993) were run in relatively deep water. Details of inshore wave conditions were not given, but it may be appropriate to assume that inshore wave conditions were similar to the offshore conditions. Using Franco's relationship between Q# and R_c/H_{si} for a vertical wall, equation (1), the overtopping for a simple vertical wall may be predicted with a = 0.2 and b = -4.295. Results for Series 1000 are plotted against Franco's equation in Figure 20. Franco's formula underestimates the overtopping discharge, particularly at larger values of R_c/H_{si}. The difference may be due to the relatively small range of relative freeboards, $0.9 < R_c/H_{si} < 2.2$, for which Franco derived the equation. In the present study a wider range of R_c/H_{si} is used in test series 1000, $0.03 < R_c/H_{si} < 3.2$. Alternative values of a = 0.03 and b = -2.05 in the Franco equation may be derived by fitting the general form of equation (1) to these test results.

It is possible that the inshore and offshore wave conditions in Franco's tests may have differed. It was not possible to investigate this directly, but HR data from Series 1000 have been re-plotted using both H_{so} and H_{si}, as shown in Figure 21. It is clear that Franco's regression line, with a = 0.2 and b = -4.295, lies below data plotted using H_{si}, but above and closer to data plotted using H_{so}. These results confirm the importance of establishing the inshore wave height with confidence, but further work will be required to extend this analysis.

Overtopping measurements by De Waal (1994) can also be compared with the prediction lines derived from Series 1000. However, De Waal's inshore wave conditions were not measured directly, but were calculated. These data are plotted against Owen's equation using A = 0.002 and B = 26.76 derived for Series 1000, in Figure 22, with good agreement.

A similar exercise has been repeated using Franco's relationship between Q# and R_c/H_{si}, again for De Waal's test results. The scatter of the data appears a little wider, but equation (1) with a = 0.03 and b = -2.05 gives good agreement with De Waal's data. This is shown in Figure 23.

5.1.3 Summary of results for vertical wall

Measurements of mean overtopping discharge for a simple vertical wall on a 1:50 bed slope have been plotted against the general form of Owen's equation, and this gave good agreement with:

$$Q^* = A \exp(-B R^*) \quad \text{with } A = 0.002 \text{ and } B = 26.76 \qquad (4)$$

The same measurements have been plotted against the general form of Franco's equation, with good agreement for:

$$Q\# = a \exp(b\, R_c/H_{so}) \quad \text{with } a = 0.03 \text{ and } b = -2.05 \qquad (5)$$

Results from completely independent tests in the Netherlands, by De Waal, have also been plotted against both equations (4) and (5), again with relatively good agreement.

5.2 Wave screens / perforated caissons

A number of wave screen / perforated caisson configurations have been investigated, and the main structural variables are summarised in Table 1. All perforated screens had a porosity of n_a = 20%. Two hole sizes of 25mm and 50mm were used, equivalent to the screen thickness and twice the screen thickness, t_s.

In considering the overtopping performance of each structural configuration tested, both Owen's and Franco's methods were explored, but the best agreement was found with Owen's method. The mean overtopping discharge for each test has therefore been used to calculate values of Q* and R*, in each instance, using the inshore wave height, H_{si}. These have been plotted as lnQ^* against R^* for each configuration in Figures 24 to 27.

The results for single and double screens, Series 2100 and 3100 / 3200, have been combined in Figure 24 as they show very close agreement. It is interesting to note that Allsop et al (1994) also found relatively little difference in the reflection performance of these configurations. The overtopping of the perforated caisson sections is, however, significantly lower than that for the simple vertical wall, summarised in Figure 24 by equation (4). This improvement is illustrated by fitting an equation of this form to the results from test Series 2100, 3100, and 3200:

$$Q^* = A \exp(-B R^*) \qquad \text{with } A = 0.005 \text{ and } B = 59.95 \tag{6}$$

The effect of changing the hole size, D_h, from $1.0t_s$ to $2.0t_s$, without changing the porosity, n_a, is shown in Figure 25. The results for the larger holes are plotted against the regression line for the smaller holes, equation (6). The change in the screen hole size does not appear to give any significant change in overtopping performance.

A more confusing picture arises when the performance of perforated caissons of different widths are compared. The perforated caisson structures considered so far were all of B_w = 0.575m. The width of the interference chambers tested in Series 2200 and 3300 were reduced to B_w = 0.400m. The overtopping results, shown in Figure 26, when compared with those for the wider chambers in Figure 24, appear to indicate a further reduction in the overtopping discharge over the whole of the parameter range tested. This somewhat surprising result suggests that the spacing B_w may have a significant affect on the overtopping discharge, which is not accounted for in other parameters. It was noted that the analysis of wave reflections from these structures by Allsop et al (1994) indicated that the reflection coefficient C_r is well correlated with the relative screen spacing to local wave length B_w/L_s. Careful examination of the results shown in Figures 24 and 26 did not, however, identify any such clear trend.

In Series 5000 and 6000, the tests explored the influence of restricting the (vertical) depth of the chambers, in double screen caissons, by raising the floor level of the chambers. This may be necessary in the prototype to ensure that there is sufficient volume of fill material to generate the weight force required to resist sliding or overturning.

In the model, impermeable material was placed in the base of each chamber of the caisson to act as ballast. The overtopping results are shown in Figure 27. At high water levels, the raised floor had relatively little influence on the size of the chamber, and hence on the overtopping performance for deep water conditions. It was expected that a reduction in the water level from +1.61m to 1.43m would reduce discharges significantly, simply by virtue of the increase in R_c and hence R^*, however, the differences are relatively small. It may therefore be concluded that the raised floors do not have a significant influence on overtopping.

At the commencement of the wave screen tests it was noted that the form of overtopping, and probably also the mean discharge, were influenced by the manner and degree of compression of the air trapped between the vertical wall, the perforated screen, and the caisson chamber roof. In preliminary tests, this effect was reduced because air was able to escape from the caisson through small gaps between the roof and side walls. These gaps were therefore sealed and the movement of air was therefore controlled by the form of the structure tested alone.

The tests were conducted under normal wave attack, $\beta = 0°$, which ensured that any escape of air from the interference chamber could be significantly restricted by the incident wave front. In the prototype, waves are unlikely to be entirely long-crested, nor will they attack perfectly at $\beta = 0°$. Any small deviations from this idealised case will allow air to escape sideways, and thus increase the dissipation within the caisson, unless this is intentionally limited by dividing the caisson internally into small separate cells. It is therefore likely that these tests give an upper limit to the overtopping performance, and overtopping will be further reduced under oblique or short-crested wave attack.

5.3 Rock armour slopes

Previous work has indicated that the addition of an rock armoured slope in front of a vertical wall might increase overtopping, by increasing the likelihood of wave run up over the slope. This may be the case if the armour is relatively impermeable to wave action, but the measurements, shown in Figure 28, provide reassurance that the armoured sections, which were tested, produced overtopping which was not higher, and was often well below, that predicted by Owen's equation, with values of A and B for the slope angle of the armour, ie. 1:1.5, and a roughness factor $r = 0.50$. Comparing the measurements for these composite structures in Figure 28, using $r = 0.50$ for a simple armoured slope in equation (3), gives close agreement at low values of R^*, when overtopping is relatively insensitive to the structure. At values of $R^* < 0.11$, the overtopping performance of the composite structure is somewhat better than would be predicted for a simple armoured slope.

A comparison can also be made with the prediction line derived earlier for the simple vertical wall, test Series 1000. At low R^* values, overtopping of the composite armoured section is again comparable to that of the vertical wall predicted by equation (4). At higher values of R^*, $R^* < 0.11$, and particularly at relatively low water levels, the overtopping performance of the armoured slope and wall are significantly better than that of the vertical wall alone. The rock armour is therefore more efficient because it dissipates wave energy as it runs up the slope.

A weakness of this simple approach is shown by the sudden drop in dimensionless overtopping parameter Q^* for those tests with $R^* < 1.1$. There is probably an influence of the relative armour crest freeboard, A_c, which has not been identified separately.

6 *Discussion of water surface conditions*

This chapter discusses a new analysis approach to describe the water surface condition. It has been developed to identify more clearly the effect of 'low-reflection' structures on the sea surface in front of breakwaters, and other potentially reflective harbour structures. It is the sea surface condition which has a significant effect on vessel navigation, especially for small craft.

Previously used methods of analysis, such as those related to the reflection coefficient, do not clearly identify the influence of the structure on the sea surface. However, some guidance on creating an analysis method for the sea surface was provided by Klopman and van der Meer (1994). They developed a procedure which describes the spatial variations of the local wave heights, as functions of the relative distance seaward from a structure. While the variation of wave height may be relevant to some types of vessels, which may have to navigate close to such a structure, a more important factor is the combination of wave height and period. Hence, the analysis method of Klopman and van der Meer (1984) was adapted to enable the spatial variation of wave steepness to be described, as a function of the relative distance from a structure.

This new technique involves the determination of the wave steepness at each of the wave probes which were positioned seaward of the structure, as described in Section 2.3.1. The steepness was calculated as follows:

$$s_m(x) = H_s(x) / L_h$$

Where: $s_m(x)$ is the mean steepness at probe position, 'x' metres from the structure

$H_s(x)$ is the significant wave height at probe position, 'x' metres from the structure

L_h is the wave length, calculated for the mean wave period, measured at the probe position ('x' metres from the structure) and the still water depth at the probe position, using the Hunt (1979) approximation to the wave dispersion equation.

The results of this analysis are presented in Figures 29 to 32, for the following structural arrangements:

- a simple vertical wall
- a single chamber wave screen, with B_w/L_s of 0.575m and a hole diameter equal to the screen thickness
- a double chamber wave screen, with B_w/L_s of 0.575m and a hole diameter equal to the screen thickness
- a rock slope, with a 1:1.5 slope and a crest level of +1.71m.

In these figures the mean wave steepness at each probe is presented as a dimensionless variable which describes the change in wave steepness compared with the incident steepness, s_{mi}, known as the relative sea steepness and defined as $s_m(x)/s_{mi}$. These values are plotted against the relative distance seaward of the structure, defined as x/L_h. Different symbols have been used for each of the three incident wave steepness, 0.02, 0.04 and 0.06.

In general the results show that at distances greater than five wave lengths seaward of the structure, the ratio of relative wave steepness closely matches that expected for reflected wave heights. The results of the tests showed that at these distances from the structure the local wave periods were comparable with the incident wave period.

However, some of the structures which were tested demonstrated significant differences in the spatial variation of sea surface steepness, even where the overall reflections, given by C_r, were relatively similar. As discussed in Chapter 4, an examination of the reflection performance of the structures which were tested, showed the effectiveness of using a single chamber wave screen. However, these results also showed that the use of a 1:1.5 rock slope provided a better overall reflection performance, and there was only a marginal difference between the more expensive option of a double chamber wave screen compared with the single chamber version.

A comparison of the relative steepness, resulting from the use of each structure, for distances greater than three wave lengths from the structure, produced the following results:

- the double chamber wave screen produced the most favourable conditions with a mean relative steepness of 1.15.
- the 1:1.5 rock slope provided only marginally worse sea surface conditions, with a greater overall relative steepness of 1.19.
- the single chamber wave screen provided a relative steepness of 1.22, which illustrates the potential benefits of the double chamber wave screen. Within the range of these results, the double chamber arrangement showed a 10% improvement in relative wave steepness over the single chamber version.
- the vertical wall produced a mean relative steepness of 1.41, which forms the upper boundary of these results.

These results demonstrate the benefits of using a double chamber wave screen over the single chamber arrangement, if such a low value of relative sea steepness is required. It also reinforces the reflection analysis results for the use of rock armour slopes, although, as previously discussed by McBride et al (1993), it is often necessary to maintain the vertical nature of the structure, which for a rock armour slope is not possible.

This analysis also indicated the spatial variability of the sea surface steepness at distances of less than three wave lengths from the structure. In this region, the results for the vertical wall, Figure 29, show that the wave steepness is rapidly changing. For this case the relative sea steepness often exceeds 1.5, which, for an incident sea steepness of 0.04 would lead to very steep waves and frequent wave breaking. These conditions will be hazardous for vessel navigation, especially small craft such as small fishing vessels or leisure craft. The results for the single chamber wave screen (Figure 30) show a similar variation in this region, though the overall mean steepness is lower than for the vertical wall arrangement. The structures which create the best conditions in this region are the double chamber wave screen (Figure 31) and the rock slope (Figure 32). The rock slope reduces the local sea surface steepness, close to the structure, to less than the incident steepness due to the distance that the slope extends from the vertical wall of the structure and the energy dissipation caused by the rough and porous layers. Obviously, it would be hazardous for vessels to navigate very close to this type of structure due to the risk of grounding.

The results of this analysis are summarised in Table 5, with corresponding values of C_r for comparison.

7 Scale effects

The use of hydraulic model test results should always be subject to analysis of the potential influence of scale effects. Such effects are principally of concern where flows in conduits or porous layers may be unrealistically influenced by viscous flow effects. In the testing of coastal structures, the most frequent concern is for the effects that any distorted flows would have on the stability of armour units. Potential scale effects have been discussed by many authors. Owen & Allsop (1983) and Owen & Briggs (1985) reviewed previous studies at laboratories in the USA, Denmark, and UK, and concluded that scale effects in the flow in the primary armour on rubble breakwaters will be very low provided that the armour unit Reynolds number, defined in terms of the nominal unit diameter, is kept above approximately $Re = 3x10^4$, or perhaps above $Re = 3x10^3$. For the current set of tests, in Series 7000 and 8000, the significant wave heights were greater than or equal to 0.1m, and the size of the rock armour was approximately 0.07m. This implies that $Re > 6x10^4$, which is well above either of the limits.

A similar argument may be pursued for flow in the holes in the perforated wave screens, where the Reynolds number may be defined in terms of the screen thickness, t_s. In these studies the lowest value of Re is given by $Re \approx 2x10^4$. This is well above a lower limit of $Re > 3x10^3$ which might be postulated from the studies on flow in porous layers, and very close to the more severe limit of $Re > 3x10^4$. Such an analogy is however a little weak on its own, so data from previous studies at HR Wallingford have been analysed for potential scale effects.

Site specific studies concerning the performance of a perforated wave screen in a large wave disturbance model, explored potential scale effects by determining the lowest wave height in the model below which levels of energy dissipation start to change significantly. This was identified by plotting the sum of relative reflected and transmitted wave energies ($C_t^2 + C_r^2$) against model wave height, see Figure 33. For model wave heights above $H_s = 0.02$m, equivalent to $Re = 4x10^3$, the energy dissipation response is flat, but begins to rise for $H_s < 0.02$m, when $Re < 4x10^3$. This is caused principally as the flow resistance of the screen increases producing greater reflections and less relative dissipation within the screen. This limit is very close to the lower limit postulated earlier, and substantially below the lower value of Re calculated for these studies. Viscous scale effects are therefore unlikely to influence any conclusions drawn from these studies.

8 Conclusions and Recommendations

8.1 Conclusions

8.1.1 Reflection analysis

- Reflections from simple vertical walls generally fall close to $C_r = 0.90$, but may be reduced by heavy overtopping. A simple reduction factor is suggested in equation (4a).

- The use of perforated wave caissons or screens has been shown to be effective in reducing reflections from vertical walls. The reflection performance of a range of single or double chamber caissons can be described within practical engineering limits by equation (5). Coefficients for this new equation have been derived from the test results, and are given in Table 4, for a selection of structural arrangements.

- A comparison of the performance of single and double chamber wave screens shows that the reflection performance of the single chamber wave screen is marginally better for $B_w/L_s < 0.2$ and worse for $B_w/L_s > 0.2$. Any improvements in the reflections, by including a second screen, seem unlikely to outweigh the increased complexity and cost of its construction.

- The optimum diameter of circular holes in the porous front screen is equal to the thickness of the screen. The use of larger holes, with a diameter equal to twice the screen thickness, may lead to a slight degradation in reflection performance.

- Small changes in water level do not significantly effect the reflective performance of single or double chamber wave screens, provided that the chambers do not alter significantly over the water level range. The use of part-depth chambers increases reflections significantly, particularly at lower relative water levels.

- Reflections from simple armoured slopes are generally well-predicted by equation (8b), except where the armour crest is relatively low. For configurations with the armoured crest below about $A_c/D_n = 1.3$, reflections may increase significantly above those predicted by equation (8b). However, this effect may be mitigated by providing a wider armour crest, or in some circumstances by supporting the armoured slope on a part-depth caisson.

- The use of measured inshore wave heights in the analysis of these results substantially improves the correlation with prediction methods.

- A simple analysis of potential scale effects indicates that the results of these tests will not be significantly influenced by viscous scale effects.

8.1.2 Overtopping analysis

- Good correlation has been found between sets of independent measurements of mean overtopping discharge, and each set appears to be well fitted by a simple equation for the overtopping of simple vertical walls, based on the lnQ* v R* relationship derived by Owen for simple slopes.

- Revisions to the Franco formula based on Q# and R_c/H_s have been derived to describe overtopping of vertical walls, and again, these seem to show good agreement with the test data.

- Wave screens placed in front of a vertical wall significantly reduce the overtopping discharge, as well as reflections. The effect of the wave screens increases as R_c/H_s or R* increases.

- The overtopping of a vertical structure protected by wave screens, or a perforated caisson, does not appear to be significantly affected by the addition of a second interference chamber, or wave screen.

- Placement of an armoured slope in front of the vertical wall generally reduces overtopping, particularly at values of $R^* < 1.1$. When the structure freeboard is low, overtopping is close to that predicted for the simple vertical wall and an armoured slope. At lower water levels, overtopping of the composite structure is lower than predicted for an armoured slope alone, and substantially lower than that predicted for the simple vertical wall.

8.1.3 Water surface conditions

- At distances of greater than five wave lengths seaward of the structure, the ratio of relative wave steepness closely matches that expected for reflected wave heights.

- An analysis of water surface conditions at distances of more than three wave lengths from the structure demonstrated the potential benefits of the double chamber wave screen over the single chamber version.

- The relative sea steepness results for the vertical wall at distances of less than three wave lengths seaward of the structure showed that rapidly changing wave steepness leads to very steep waves and frequent wave breaking. These conditions would be hazardous for small craft navigating in this region.

8.2 Recommendations

It is recommended that further, more detailed analysis is carried out on both the overtopping and sea steepness analyses discussed in this report. This is necessary in order to provide a greater understanding of wave by wave overtopping and the spatial variation of sea steepness. The further analysis of the sea steepness results requires particular attention due to the potential impact on the navigation of small and leisure craft.

It is also recommended that further testing and analysis is carried out into all aspects of this work. In particular, it is important that a comprehensive series of 3D physical model tests are carried out to enable the effects of differing angles of wave incidence to be assessed on wave reflections, overtopping and sea steepness.

9 Acknowledgements

The work described in this report is based on work completed by members of the Ports and Estuaries, and Coastal Groups of HR Wallingford for the Construction Directorate of the Department of Environment, under research contracts PECD 7/6/263, 7/6/298 and 7/6/312, and the Department of Transport. Further testing and analysis has been supported by the European Community MAST II programme, under Sub-task 4.3 of the MCS project, and the University of Sheffield.

10 References

Allsop N.W.H. (1990) "Reflections performance of rock armoured slopes in random waves" Proceedings of 22nd ICCE, ASCE, Delft, July 1990, pp1460-1472.

Allsop N.W.H. & Beresford P.J. (1993) "Cardiff Bay Barrage Design Study - Report 10: Hydraulic modelling of caisson breakwaters" Report EX 2783, HR Wallingford, April 1993.

Allsop N.W.H. & Channell A.R. (1989) "Wave reflections in harbours: reflection performance of rock armour slopes in random waves" Report OD 102, HR Wallingford, March 1989.

Allsop N.W.H. & Hettiarachichi S.S.L. (1988) "Reflections from coastal structures" Proceedings of 21st ICCE, ASCE, Malaga, June 1988, pp782-794.

Allsop N.W.H. & McBride M.W. (1993) "Reflections from vertical walls: the potential for improvement in vessel safety and wave disturbance" Proceedings of International Workshop on Wave Barriers in Deepwaters, Port and Harbour Research Institute, Yokosuka, Japan, 10-14 January 1994, pp101-128.

Allsop N.W.H., McBride M.W., & Colombo D. (1994) "The reflection performance of vertical walls and 'low reflection' alternatives: results of wave flume tests" Paper to 3rd MCS Workshop, Emmelord, November 1994.

Allsop N.W.H. & Steele A.A.J. (1990) "Cardiff Bay Barrage Design Study - Report 2a: Performance of wave screen breakwater" Report EX 2124, HR Wallingford, April 1990.

Bennett G.S., McIver P., & Smallman J.V. (1992) "A mathematical model of a slotted wave screen breakwater" Coastal Engineering, Volume 18, Elsevier, 1992.

Besley P., Reeves M.K. & Allsop N.W.H. (1993) "Random waves physical model tests: overtopping and reflection performance" Report IT 384, HR Wallingford, February 1993.

Davidson M.A. (1992) "The development and implementation of a software routine for the analysis of the reflection process associated with random and monochromatic waves" Internal Report 001/92, Department of Civil and Structural Engineering, University of Plymouth, May 1992.

Davidson M.A., Bird P.A.D., Bullock G.N. & Huntley D.A. (1994) "Wave reflection: field measurements, analysis and theoretical developments" Proceedings of Coastal Dynamics '94, Universtat Politecnica de Catalunya, Barcelona, February 1994.

De Waal J.P. (1994) "Wave overtopping of vertical coastal structures: influence of wave breaking and wind" Paper to 2nd MCS Workshop, Milan, April 1994.

Franco L. (1993) "Overtopping of vertical faced breakwaters: results of model tests and admissible overtopping rates" Paper 1st MCS Workshop, Madrid, October 1993.

Gilbert G. & Thompson D.M. "Reflections in random waves: the frequency response function method" Report IT 173, Hydraulics Research Station, Wallingford, March 1978.

Goda Y. (1985) "Random seas and design of maritime structures" University of Tokyo, Tokyo, 1985.

Herbert D.M. (1993) "Wave overtopping of vertical walls" Report SR 316, HR Wallingford, February 1993.

Hunt J.N. (1979) "Direct solution of wave dispersion equation" Journal of Waterways and Harbours Division, ASCE, Vol WW4, November 1979. pp 457-459.

Kajima R. (1969) "Estimation of an incident wave spectrum under the influence of reflection" Coastal Engineering in Japan, Volume 12, 1969.

Klopman G. & van der Meer J.W. "Random wave measurements in front of reflective structures" Paper to 2nd MCS Workshop, Milan, April 1994.

McBride M.W., Hamer B.A., Besley P., Smallman J.V. & Allsop N.W.H. (1993) "The hydraulic design of harbour entrances: a pilot study" Report SR 338, HR Wallingford, April 1993.

McBride M.W., Smallman J.V. & Allsop N.W.H. (1994) "Design of harbour entrances: breakwater design and vessel safety" Proceedings of Hydro-port '94, Port and Harbour Research Institute, Yokosuka, Japan, 19-21 October 1994, pp525-541.

McBride M.W., Smallman J.V. & Allsop N.W.H. (1995) "Vertical walls and low reflection alternatives: numerical modelling of absorbing wave screens" Report IT 400, HR Wallingford, February 1995.

McBride M.W., Smallman J.V. & Allsop N.W.H. (1996) "Guidelines for the hydraulic design of harbour entrances" Report SR 420, HR Wallingford, February 1996.

McKenna J.E., Besley P., Allsop N.W.H. & Whittaker T.J.T. (1994) "Wave pressures on simple vertical walls and the influence of rock mounds - preliminary results of wave flume tests" Paper to 3rd MCS Workshop, Emmeloord, November 1994.

Owen M.W. (1980) "Design of seawalls allowing for wave overtopping" Report EX 924, HR Wallingford, June 1980.

Owen M.W. & Allsop N.W.H. (1983) "Hydraulic modelling of rubble-mound breakwaters" Proceedings of Conference on Breakwaters - Design and Construction, Institution of Civil Engineers, London, May 1983.

Owen M.W. & Briggs M.G. (1985) "Limitations of modelling" Proceedings of Conference on Developments in Breakwaters, Institution of Civil Engineers, London, October 1985.

Owen M.W. & Steele A.A.J. (1991) "Effectiveness of recurved wave return walls" Report SR 261, HR Wallingford, February 1991.

Seelig W.N. (1983) "Wave reflection from coastal structures" Proceedings of Coastal Structures '83, ASCE, Arlington, March 1983, pp961-973.

Tables

Table 1 Wave conditions and wave screen spacings in terms of B_w/L_s

B_w = 0.575m				B_w = 0.40m			
Water depth at structure, h_s = 0.70m				Water depth at structure, h_s = 0.70m			
$s_m \backslash H_{so}$	0.10	0.20	0.25	$s_m \backslash H_{so}$	0.10	0.20	0.25
0.02	0.14	0.09	-	0.02	-	0.07	-
0.04	0.24	0.14	0.12	0.04	-	0.10	0.09
0.06	-	0.19	0.16	0.06	-	0.13	0.11
Water depth at structure, h_s = 0.61m				Water depth at structure, h_s = 0.61m			
$s_m \backslash H_{so}$	0.10	0.20	0.25	$s_m \backslash H_{so}$	0.10	0.20	0.25
0.02	0.15	0.10	-	0.02	-	0.07	-
0.04	0.25	0.15	0.13	0.04	0.17	0.10	0.09
0.06	-	0.20	0.17	0.06	-	0.14	0.12
Water depth at structure, h_s = 0.43m				Water depth at structure, h_s = 0.43m			
$s_m \backslash H_{so}$	0.10	0.20	0.25	$s_m \backslash H_{so}$	0.10	0.20	0.25
0.02	0.17	0.12	-	0.02	-	-	-
0.04	0.27	0.17	0.15	0.04	-	0.12	-
0.06	-	0.22	0.19	0.06	-	0.15	0.13

Table 2 Test programme

Test series		Structure	B_w (m)	Water level (m flume)	Screen hole diameter	Number of tests
1000	1000	Vertical structure only	-	1.43, 1.61, 1.71	-	23
2000	2100	Vertical wall and single wave screen	0.575	1.43, 1.61, 1.71	screen thickness	23
	2200	Vertical wall and single wave screen	0.40	1.43, 1.61, 1.71	screen thickness	19
3000	3100	Vertical wall and double wave screen	0.575	1.43	screen thickness	4
	3200	Vertical wall and double wave screen	0.575	1.61	screen thickness	8
	3300	Vertical wall and double wave screen	0.40	1.61	screen thickness	8
4000	4100	Vertical wall and double wave screen	0.575	1.61	2 * screen thickness	8
	4200	Vertical wall and single wave screen	0.575	1.61	2 * screen thickness	8
5000	5100	Double screen - front and rear chamber floors at depths of 30% caisson height	0.575	1.43	screen thickness	4
	5200	Double screen - front and rear chamber floors at depths of 30% caisson height	0.575	1.61	screen thickness	5
6000	6100	Double screen - front and rear chamber floors at depths of 30% and 50% caisson height, respectively	0.575	1.43	screen thickness	4
	6200	Double screen - front and rear chamber floors at depths of 30% and 50% caisson height, respectively	0.575	1.61	screen thickness	5
7000	7100	Rock armour slope - 1:1.5 - 2 stone berm width - berm level of 1.71m	-	1.43	-	4
	7200	Rock armour slope - 1:1.5 - 2 stone berm width - berm level of 1.71m	-	1.61	-	5
8000	8100	Rock armour slope - 1:1.5 - 2 stone berm width - berm level of 1.61m	-	1.43	-	4
	8200	Rock armour slope - 1:1.5 - 2 stone berm width - berm level of 1.61m	-	1.61	-	5

Table 3 Reflections from vertical wall, Test Series 1000

Test number	Water level relative to flume floor (m)	Wave height, H_s (m)	Wave steepness, s_m	Reflection coefficient, C_r
1001	1.43	0.10	0.02	0.902
1002	1.43	0.10	0.04	0.900
1003	1.43	0.20	0.02	0.890
1004	1.43	0.20	0.04	0.890
1005	1.43	0.20	0.06	0.877
1006	1.43	0.25	0.04	0.863
1006b	1.43	0.25	0.04	0.856
1007	1.43	0.25	0.06	0.857
1007b	1.43	0.25	0.06	0.861
1008	1.61	0.10	0.02	0.886
1009	1.61	0.10	0.04	0.895
1010	1.61	0.20	0.02	0.883
1011	1.61	0.20	0.04	0.884
1012	1.61	0.20	0.06	0.868
1013	1.61	0.25	0.04	0.875
1014	1.61	0.25	0.06	0.871
1024	1.61	0.30	0.04	0.849
1023	1.61	0.30	0.06	0.858
1022	1.61	0.16	DH bi-mod	0.886
1025	1.61	0.28	HR bi-mod 1	0.844
1026	1.61	0.25	HR bi-mod 2	0.857
1015	1.70	0.10	0.02	0.875
1016	1.70	0.10	0.04	0.879
1017	1.70	0.20	0.02	0.849
1018	1.70	0.20	0.04	0.852
1019	1.70	0.20	0.06	0.833
1020	1.70	0.25	0.04	0.832
1021	1.70	0.25	0.06	0.817

Table 4 Coefficients in Equation (2) for tested screen configurations

Screen	Hole diameter	Curve	k_c	k_x	k_y
Single	screen thickness	1	910	0.225	0.280
Single	2 * (screen thickness)	2	780	0.223	0.315
Double	screen thickness	3	750	0.250	0.265
Double	2 * (screen thickness)	4	750	0.250	0.275

Table 5 Results of water surface analysis

Structure	Mean, relative sea steepness at > $3L_h$ seaward of structure	Lowest recorded C_r
Vertical wall	1.41	0.87
Single chamber wave screen	1.22	0.28
Double chamber wave screen	1.16	0.27
Rock armour slope	1.19	0.23

Figures

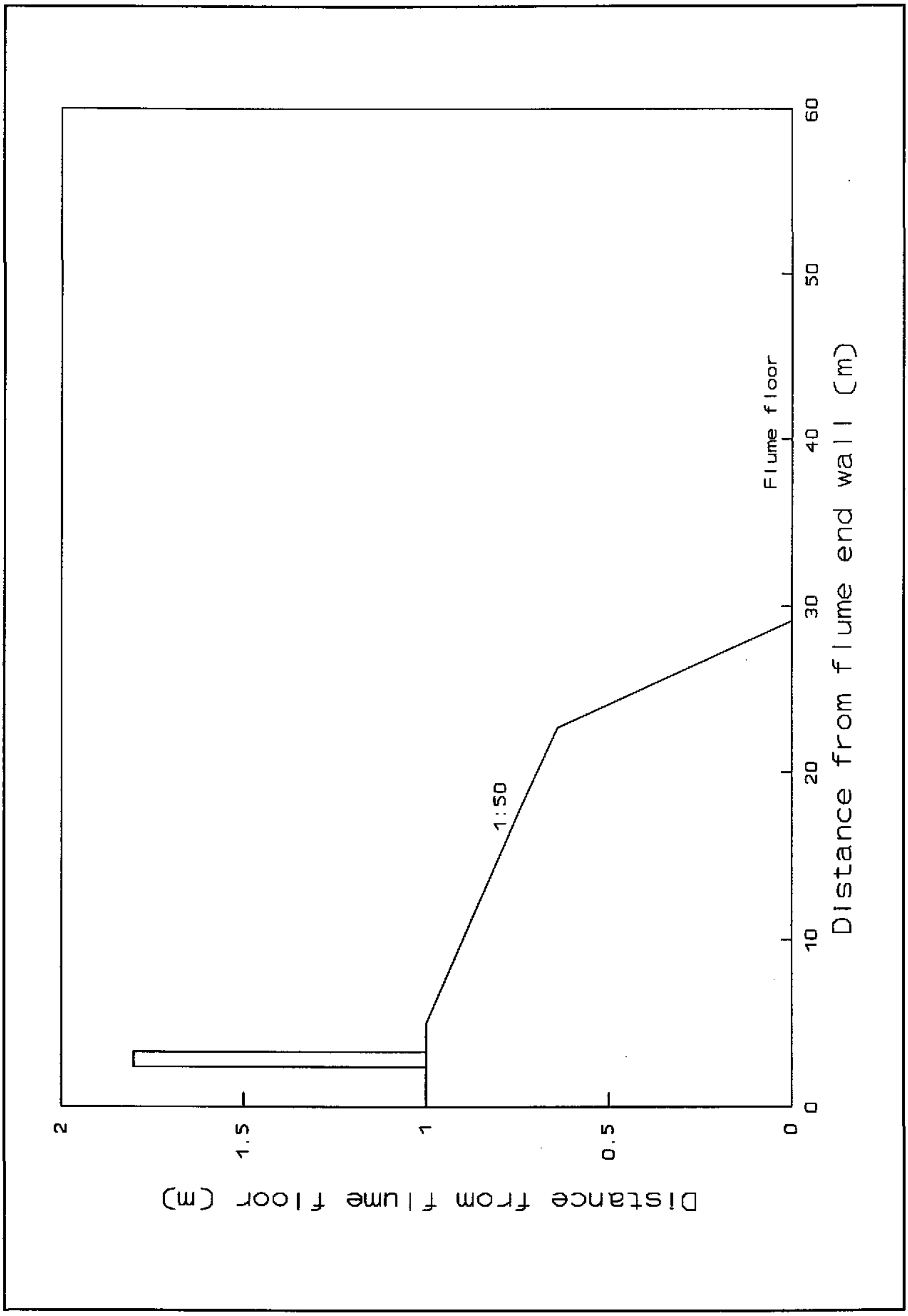

Figure 1   Model configuration with bathymetry

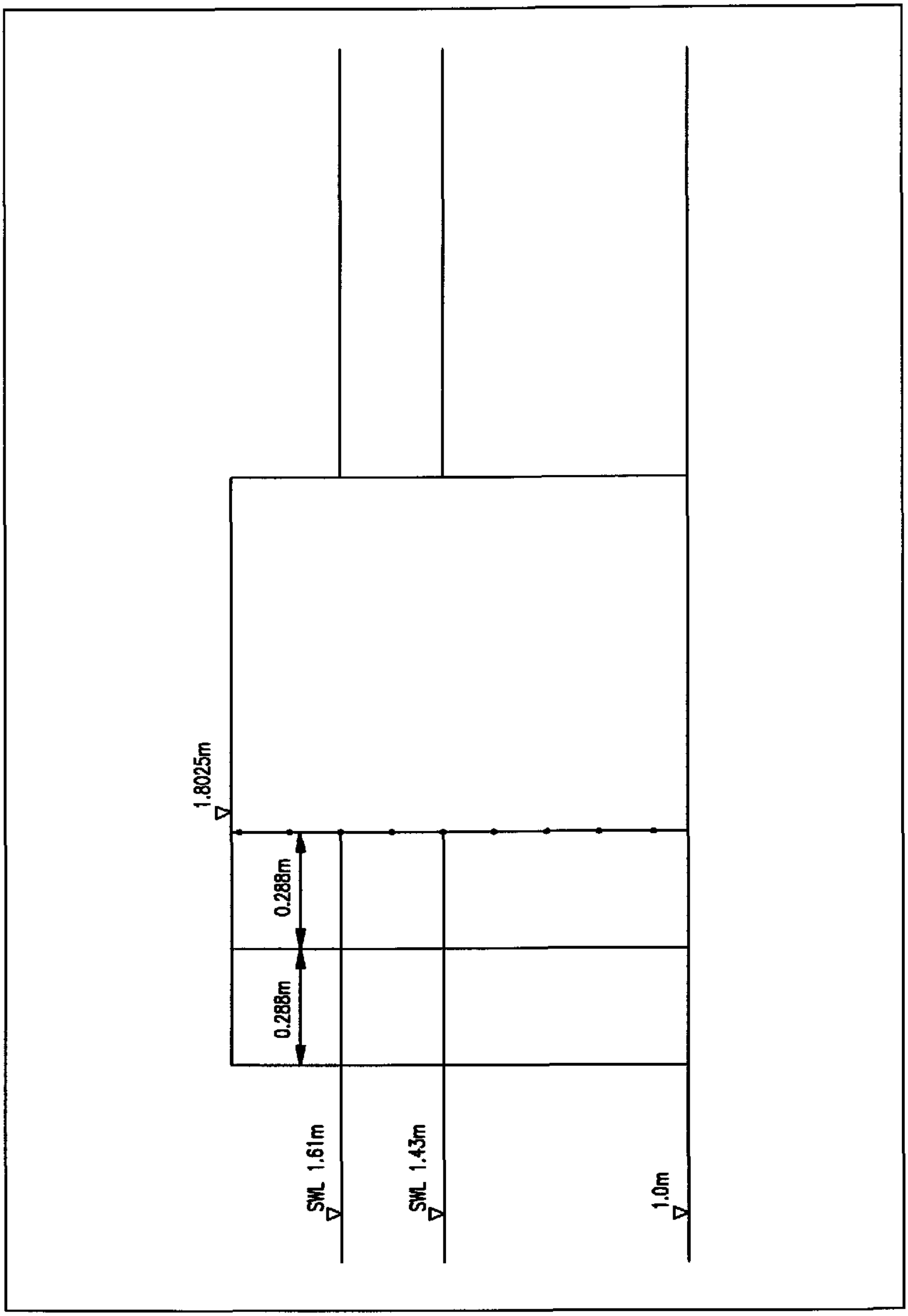

Figure 2 Model caisson with double screens at B_w=0.575m

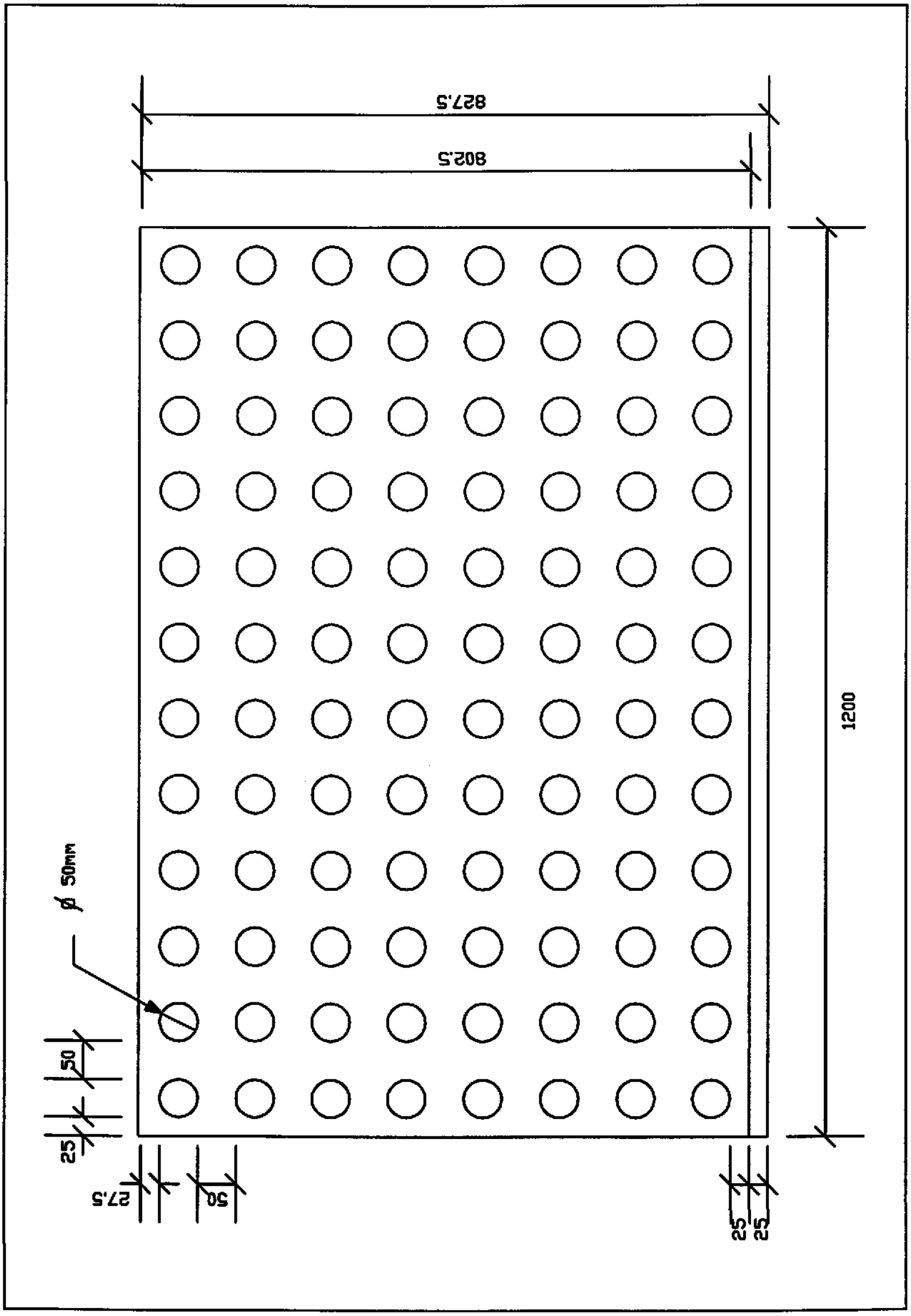

Figure 3 Perforated wave screen, n_a = 20%

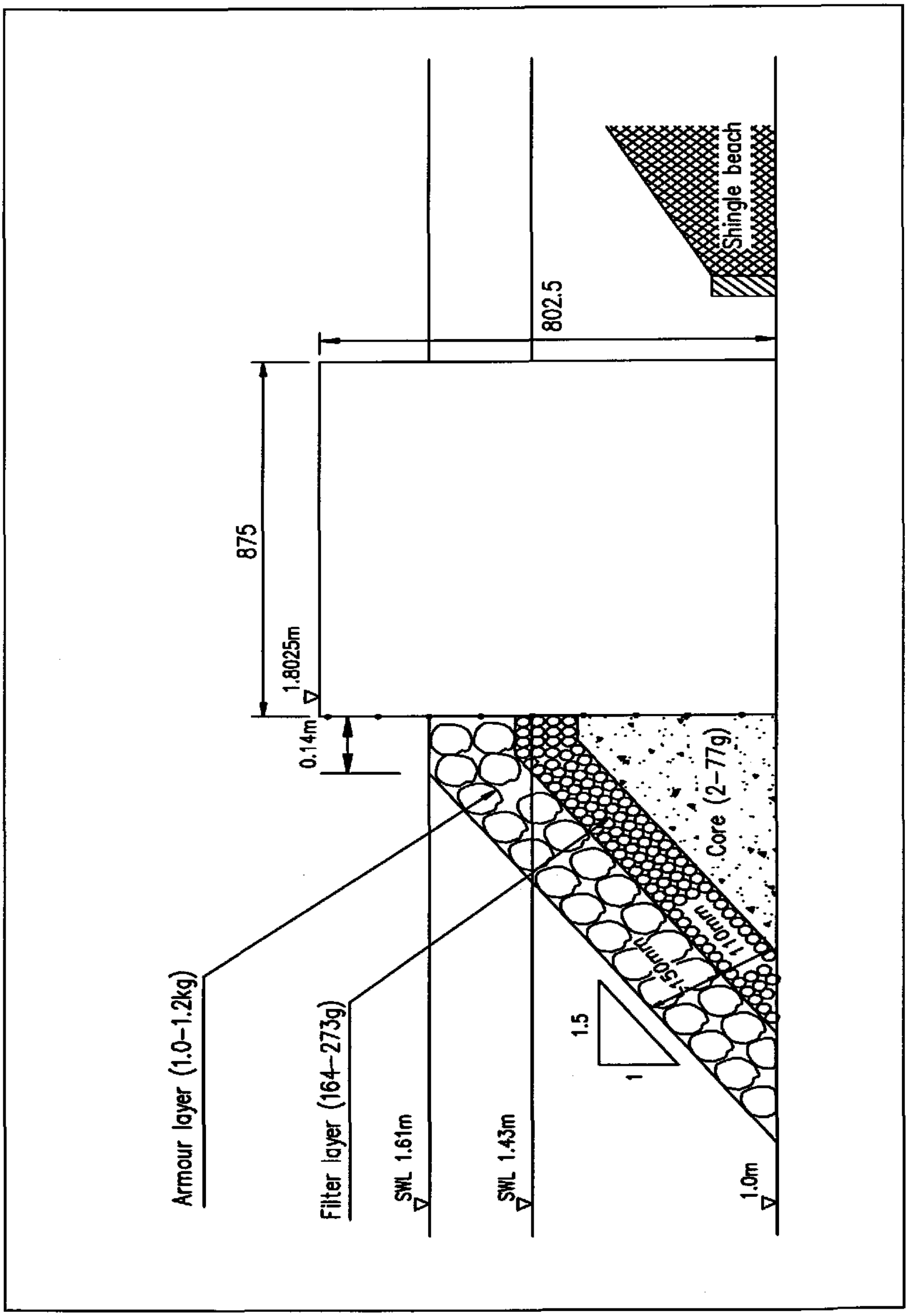

Figure 4 Vertical wall with rock armour slope

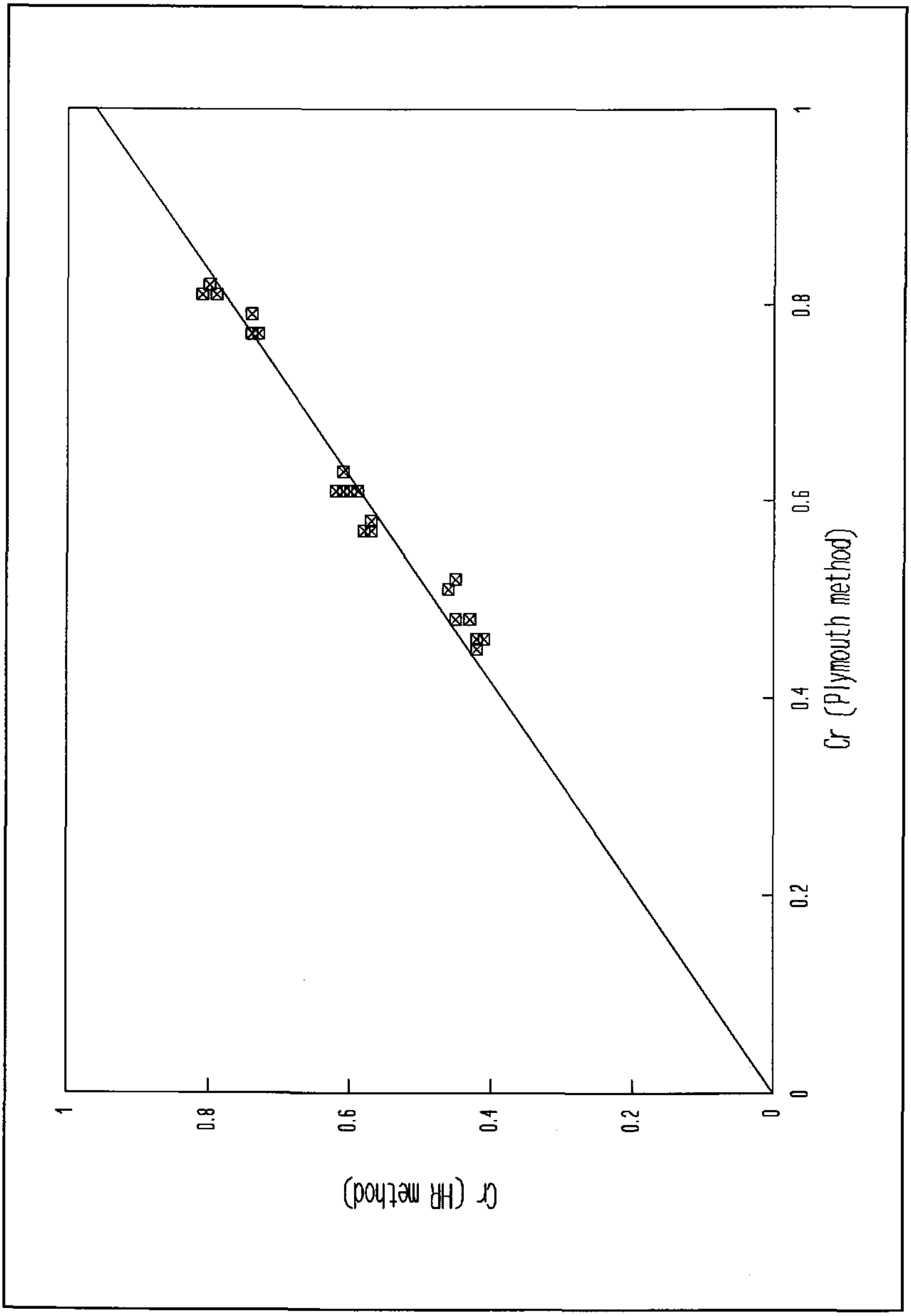

Figure 5 Comparison of reflection analysis methods

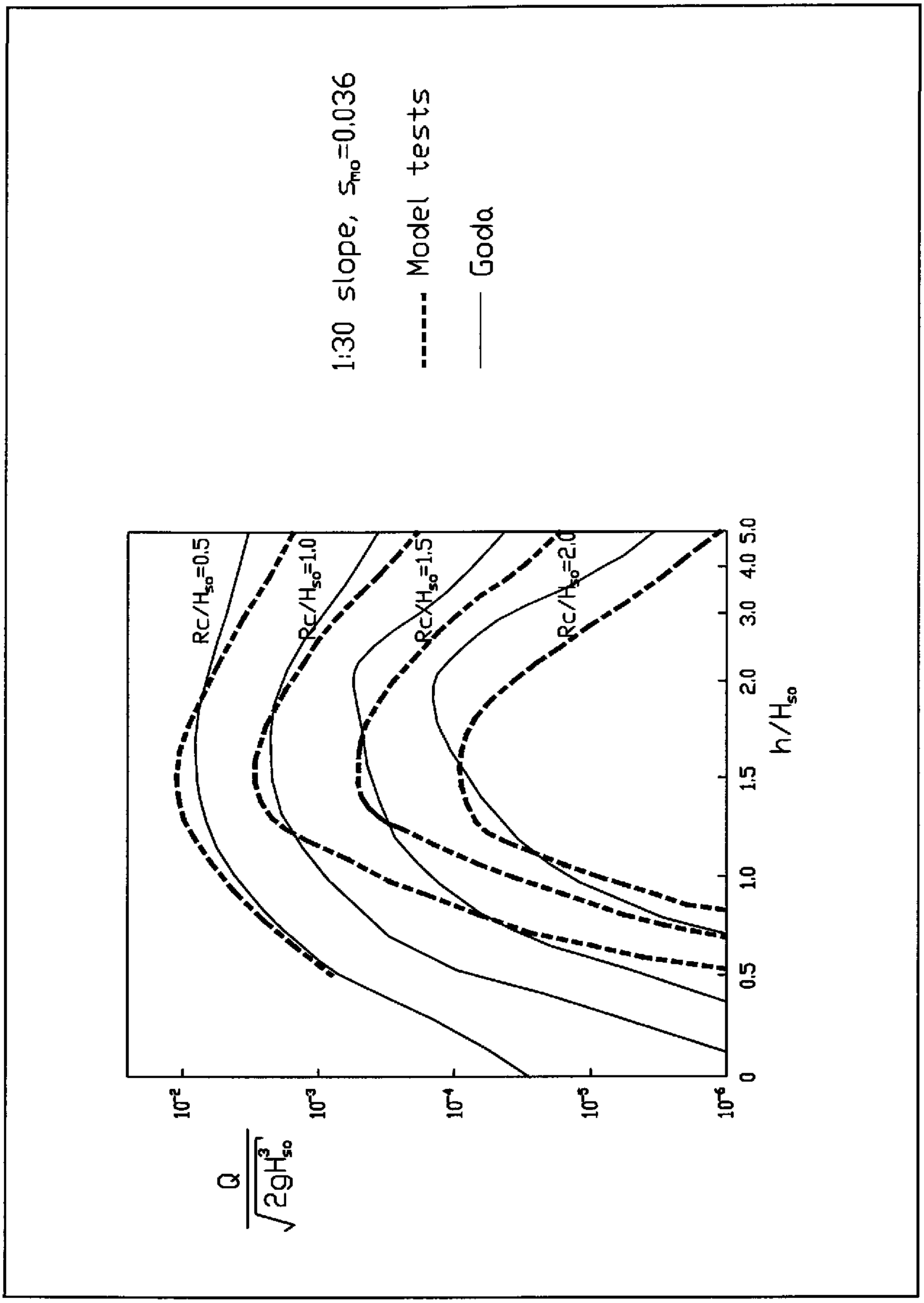

Figure 6 **Overtopping of simple vertical walls, comparison of Herbert (1993) and Goda (1985)**

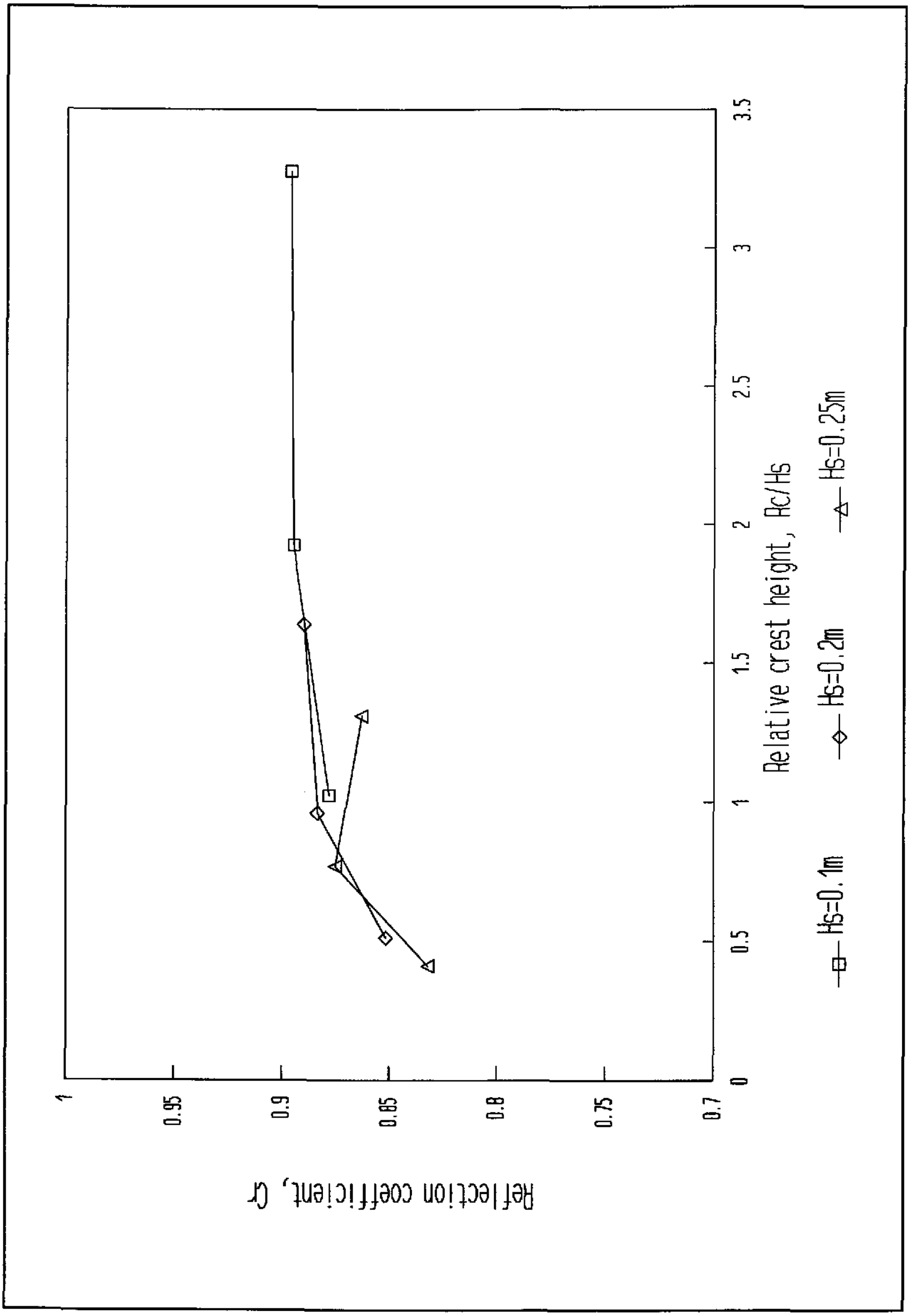

Figure 7 Influence of relative crest height on reflections

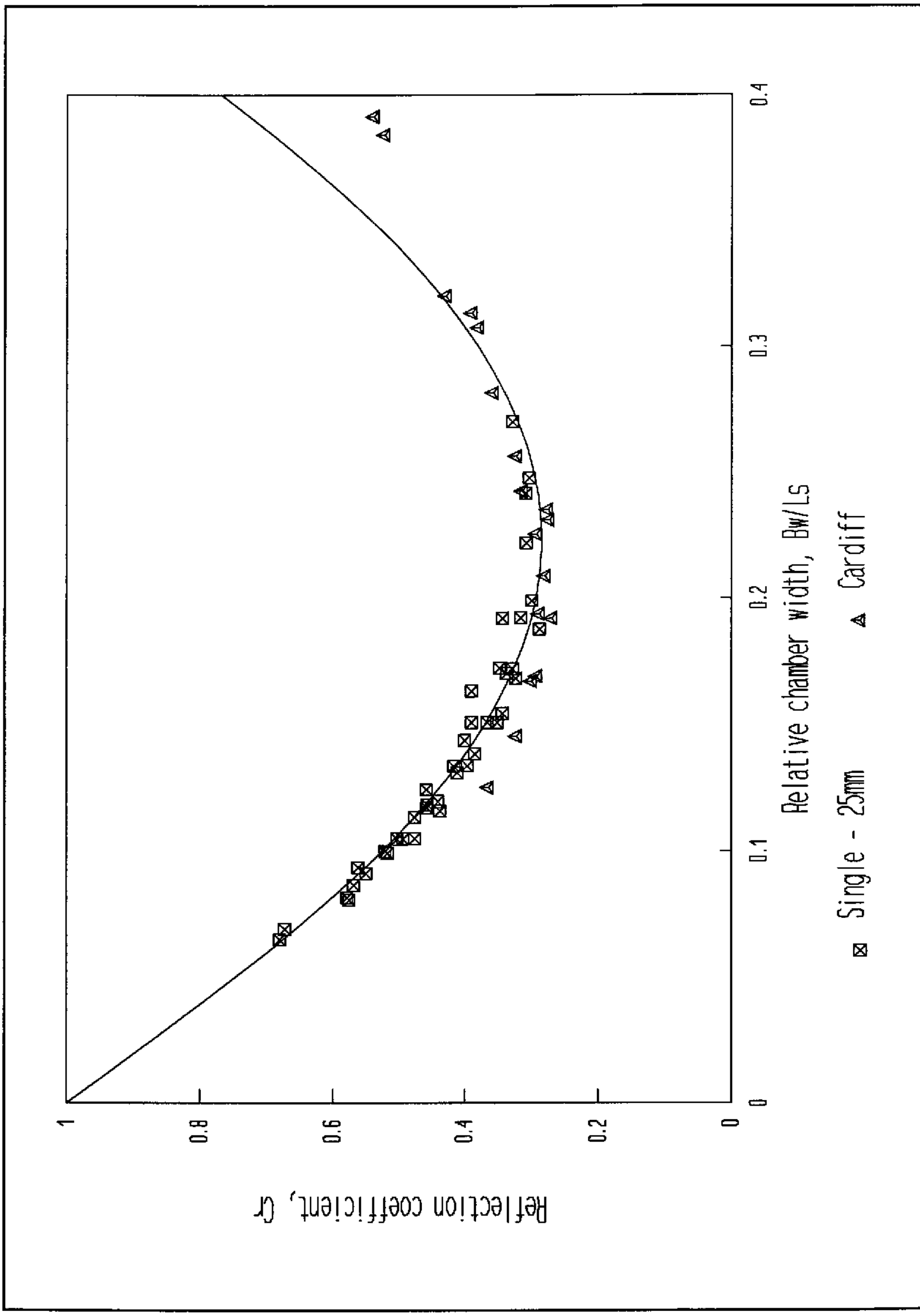

Figure 8 Reflections from single chamber with hole diameters = screen thickness, n_a=20%, curve 1, eqn (6a)

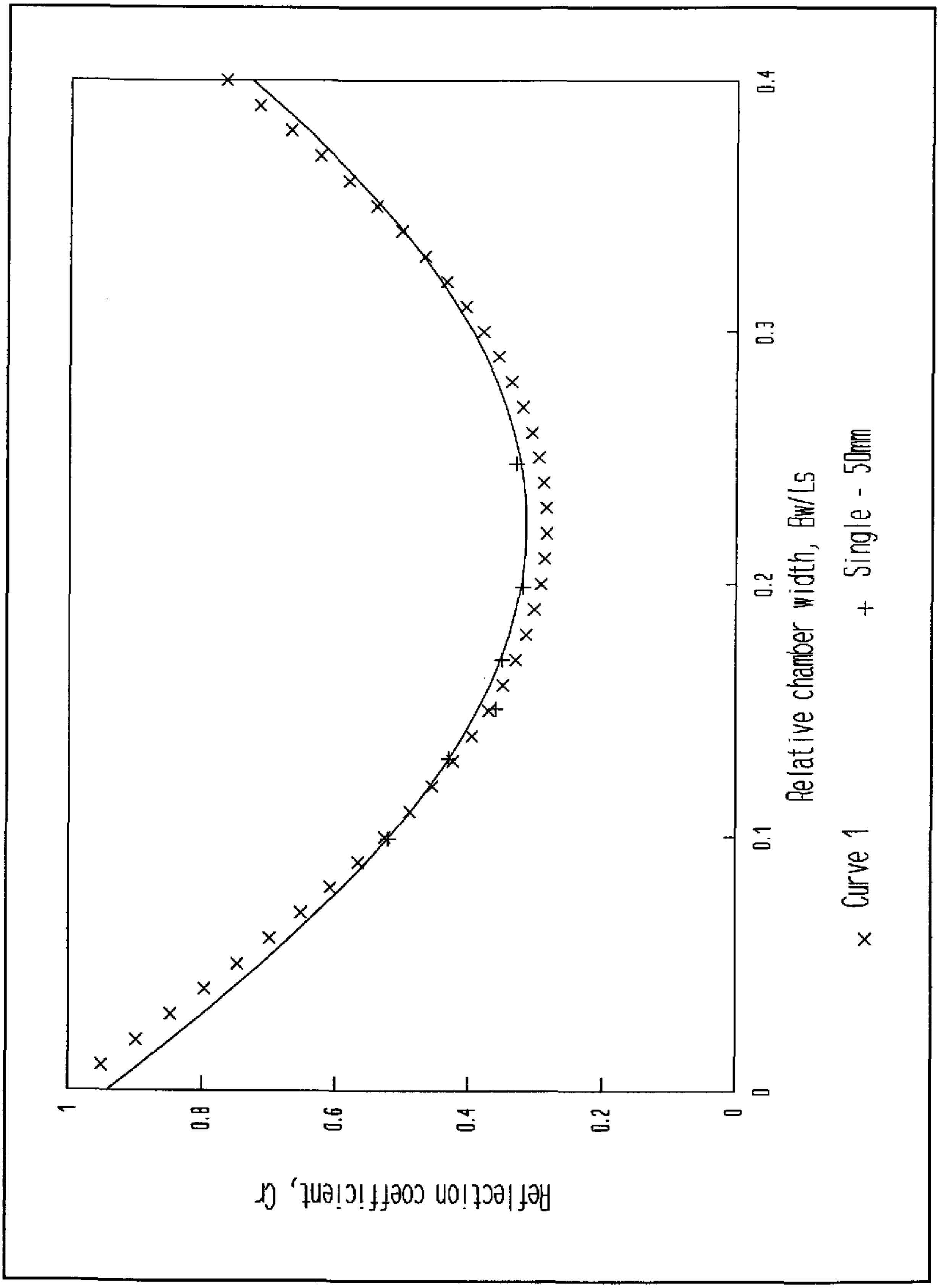

Figure 9 Reflections from single chamber with hole diameter = 2 x screen thickness, n_a=20%, curve 2, eqn (6b)

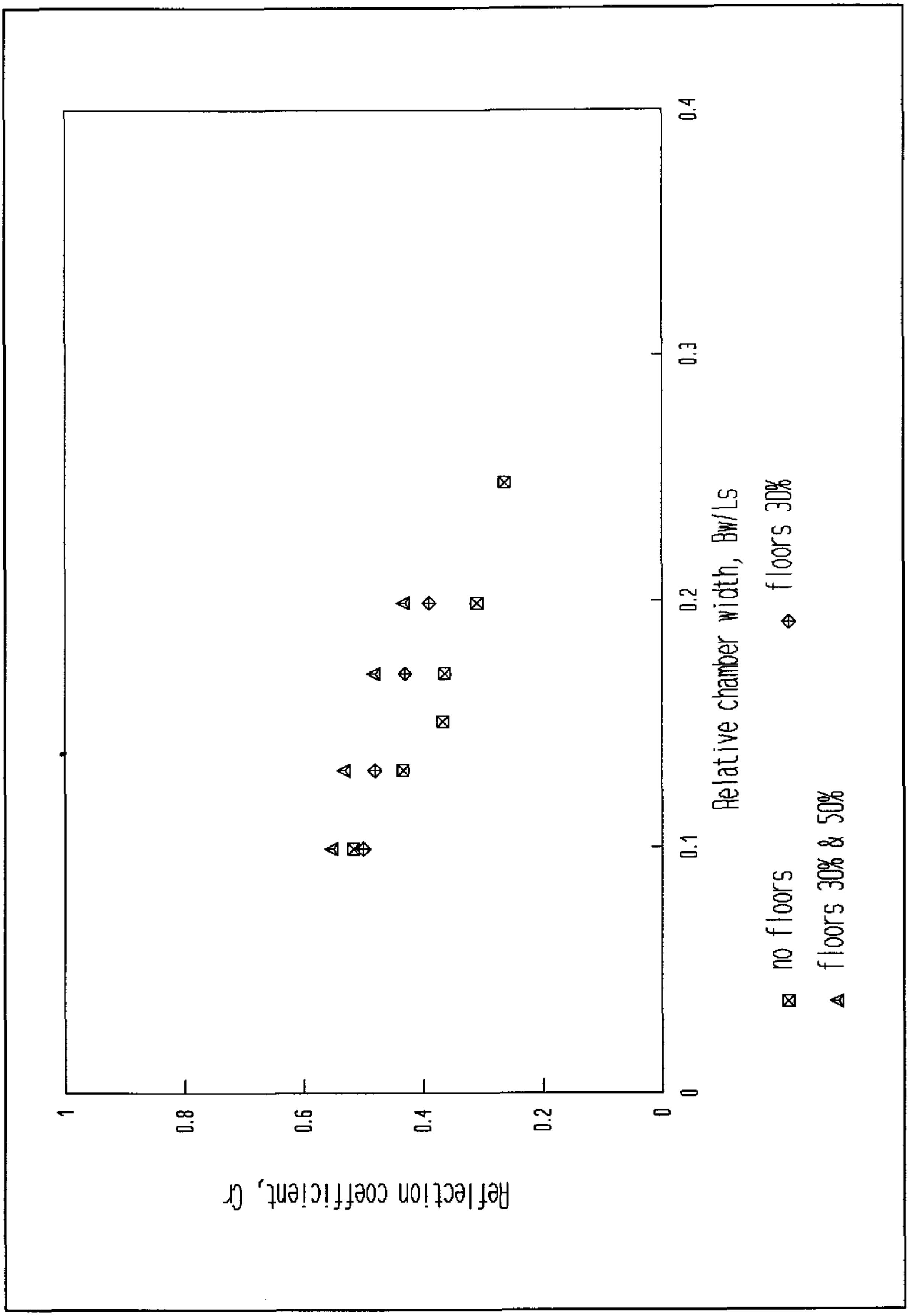

Figure 10 Influence of part-depth floors, water level at +1.61m

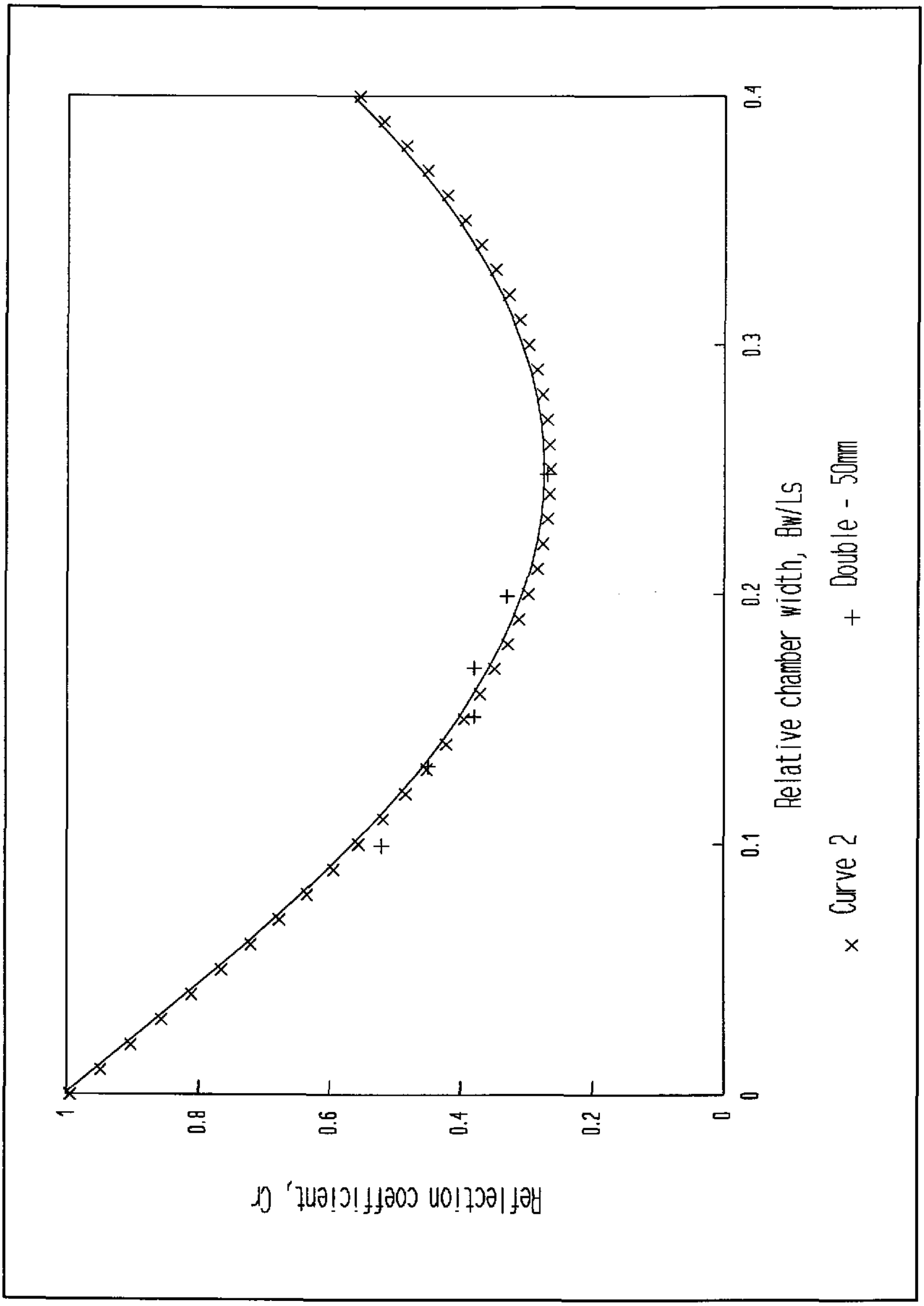

Figure 11 Reflections from double chamber with hole diameter = 2 x screen thickness, n_a=20%, curve 4

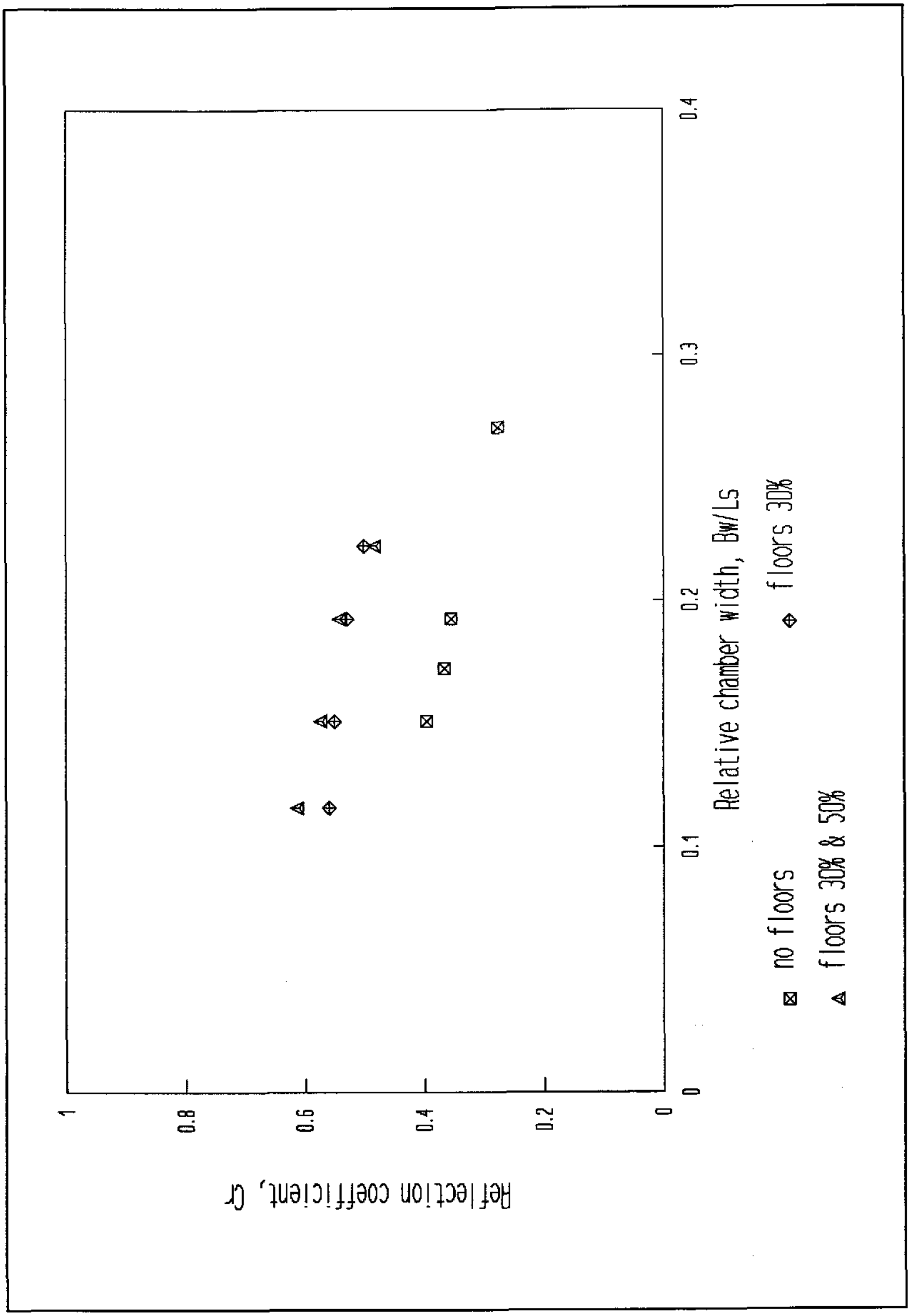

Figure 12 Influence of part-depth floors, water level at +1.43m

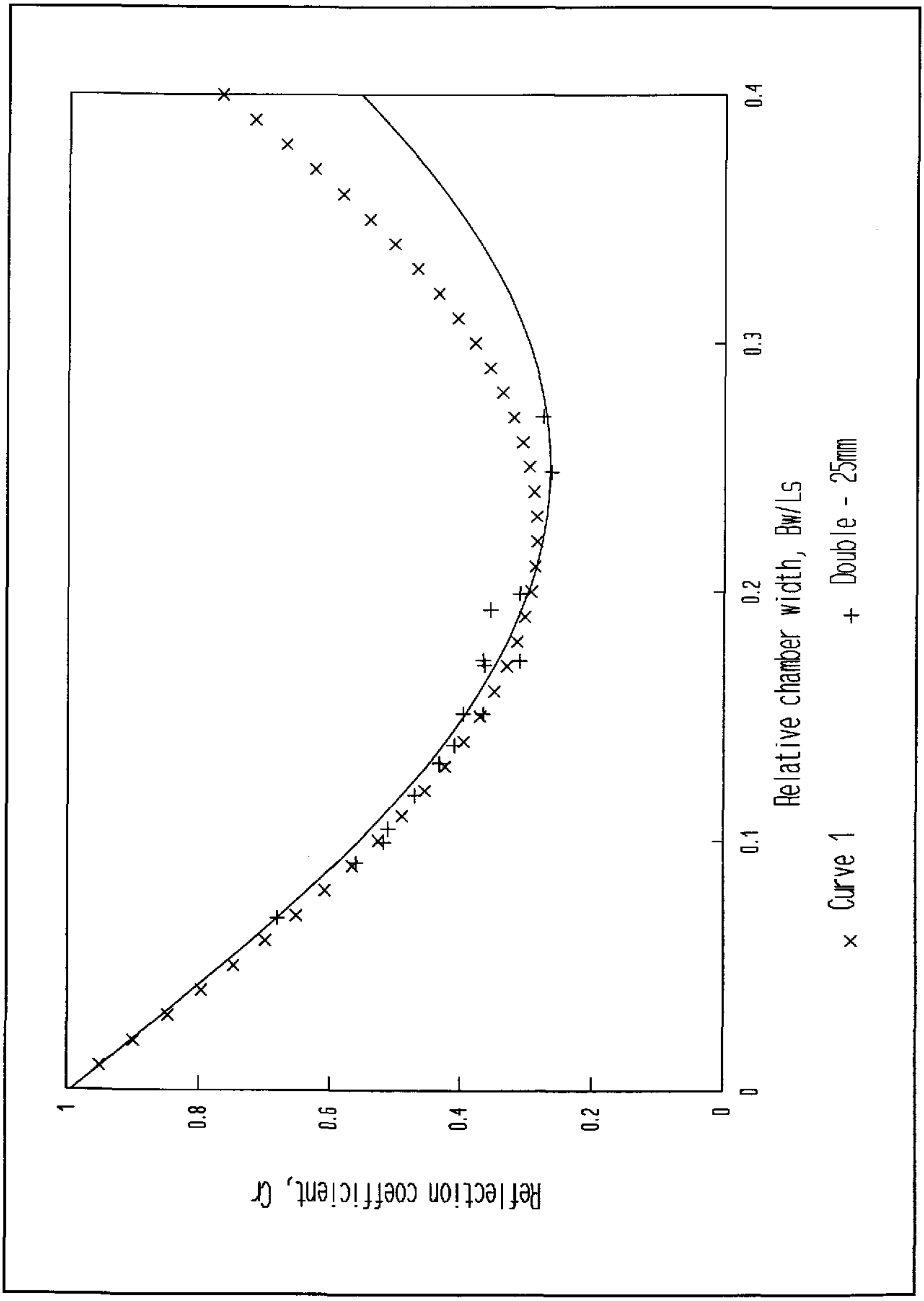

Figure 13 Reflections from double chamber with hole diameter = screen thickness, n_a=20%, curve 3

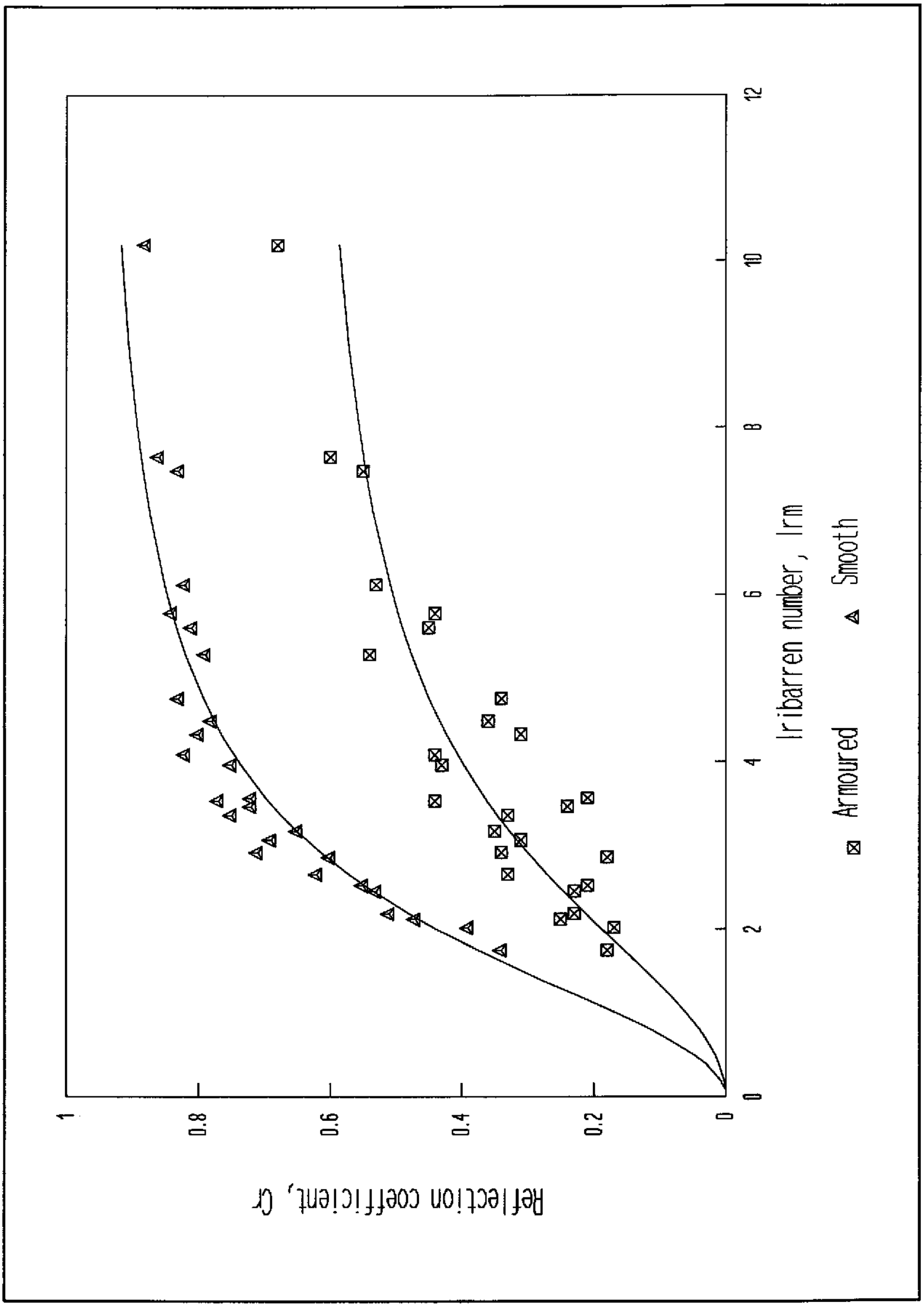

Figure 14 Reflection performance of smooth and armoured slopes, after Allsop (1990)

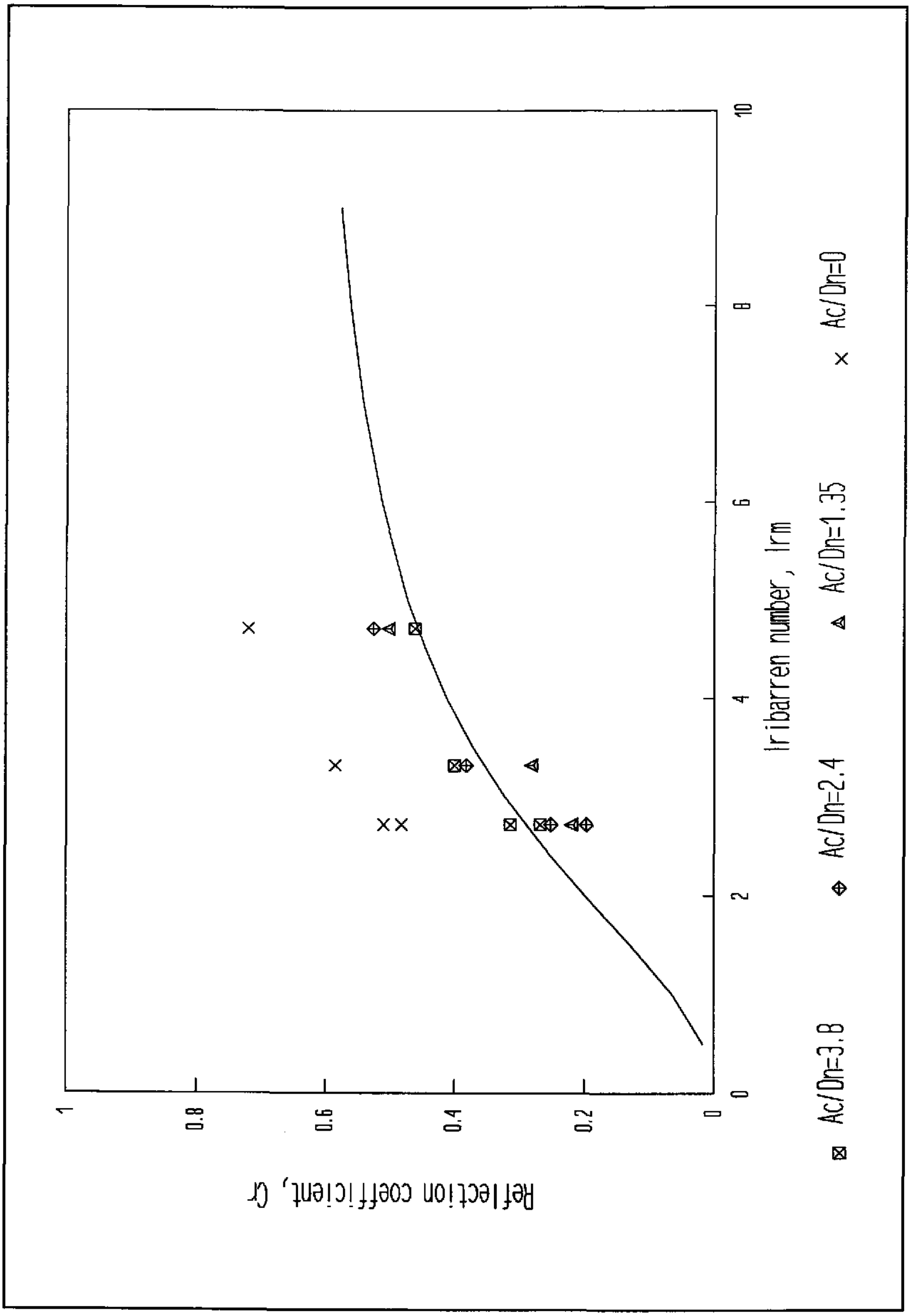

Figure 15 Reflections from armoured slopes in front of vertical wall

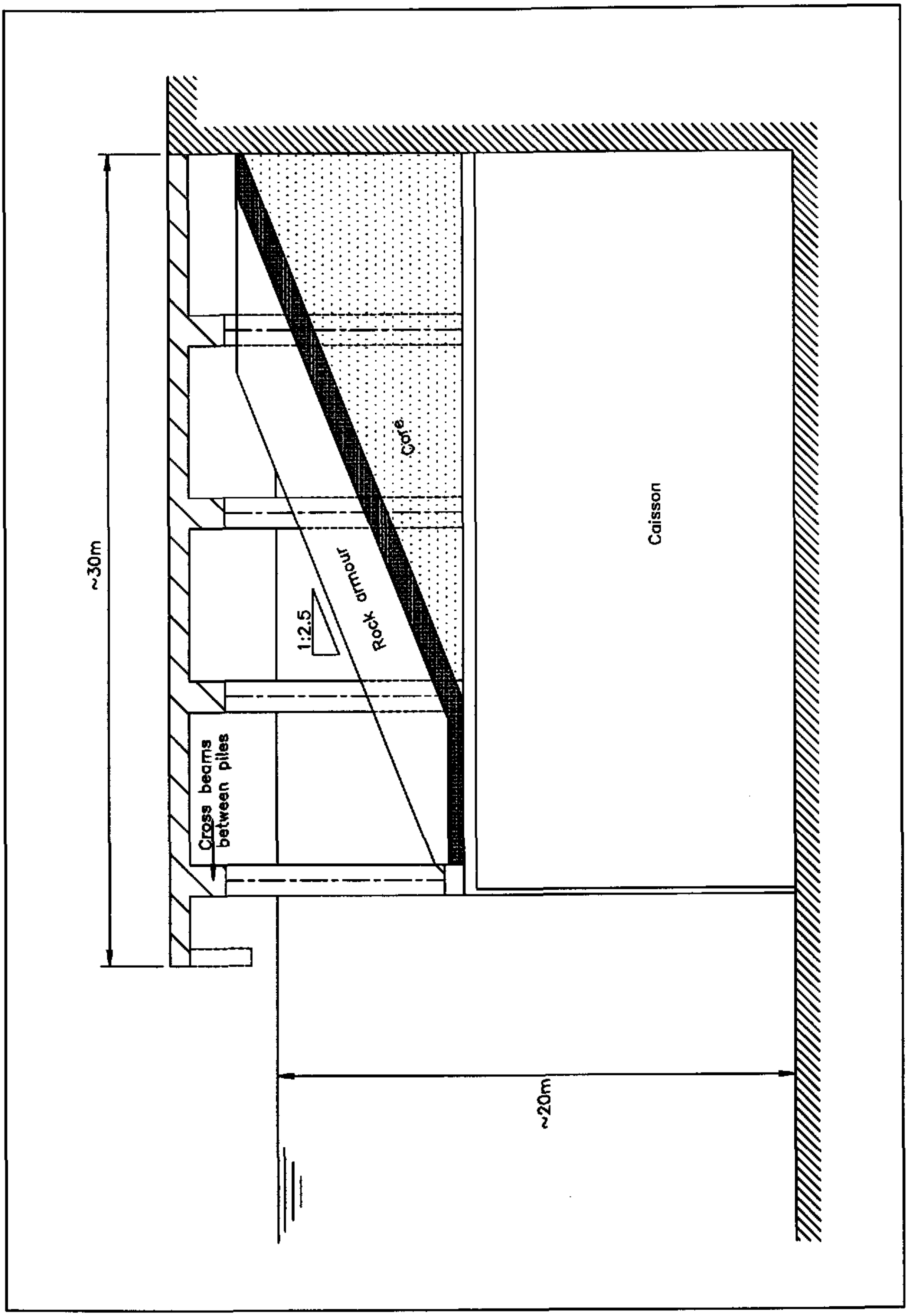

Figure 16 Piled quay over armoured slope on part-depth caisson

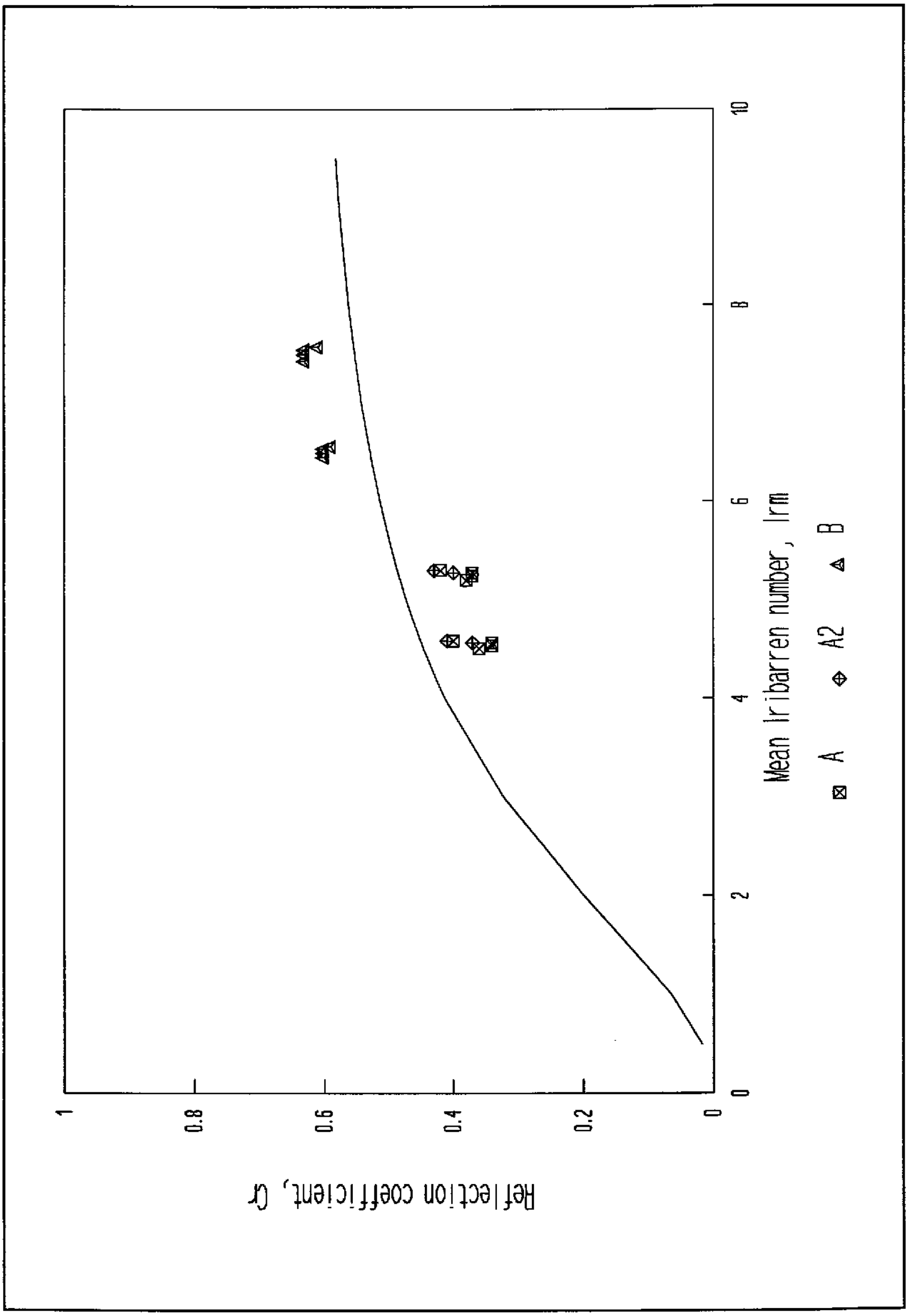

Figure 17 Reflections from alternative coal berth quays

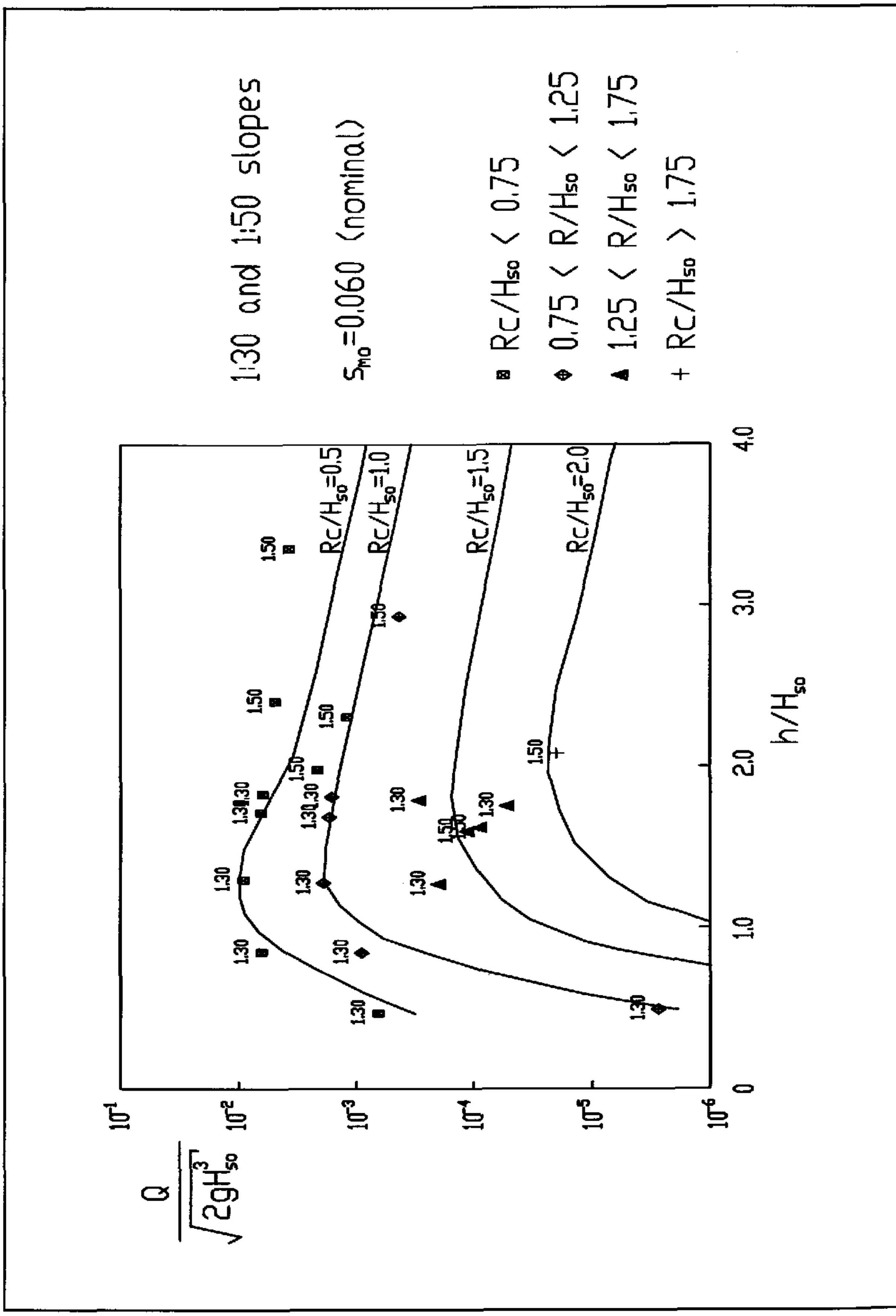

Figure 18 Comparison between Herbert's results and Series 1000

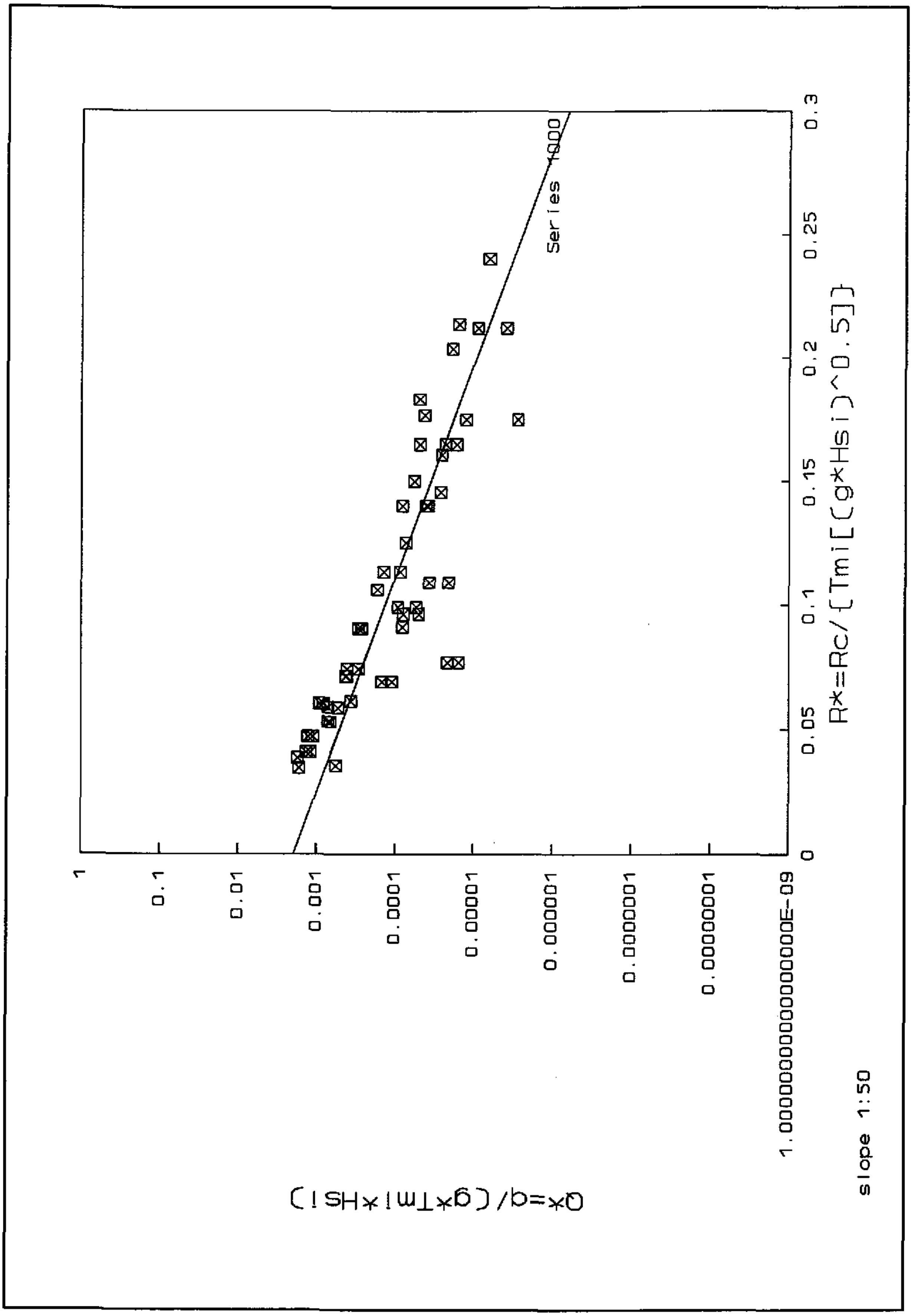

Figure 19 Simple vertical walls, Series 1000, Owen's equation

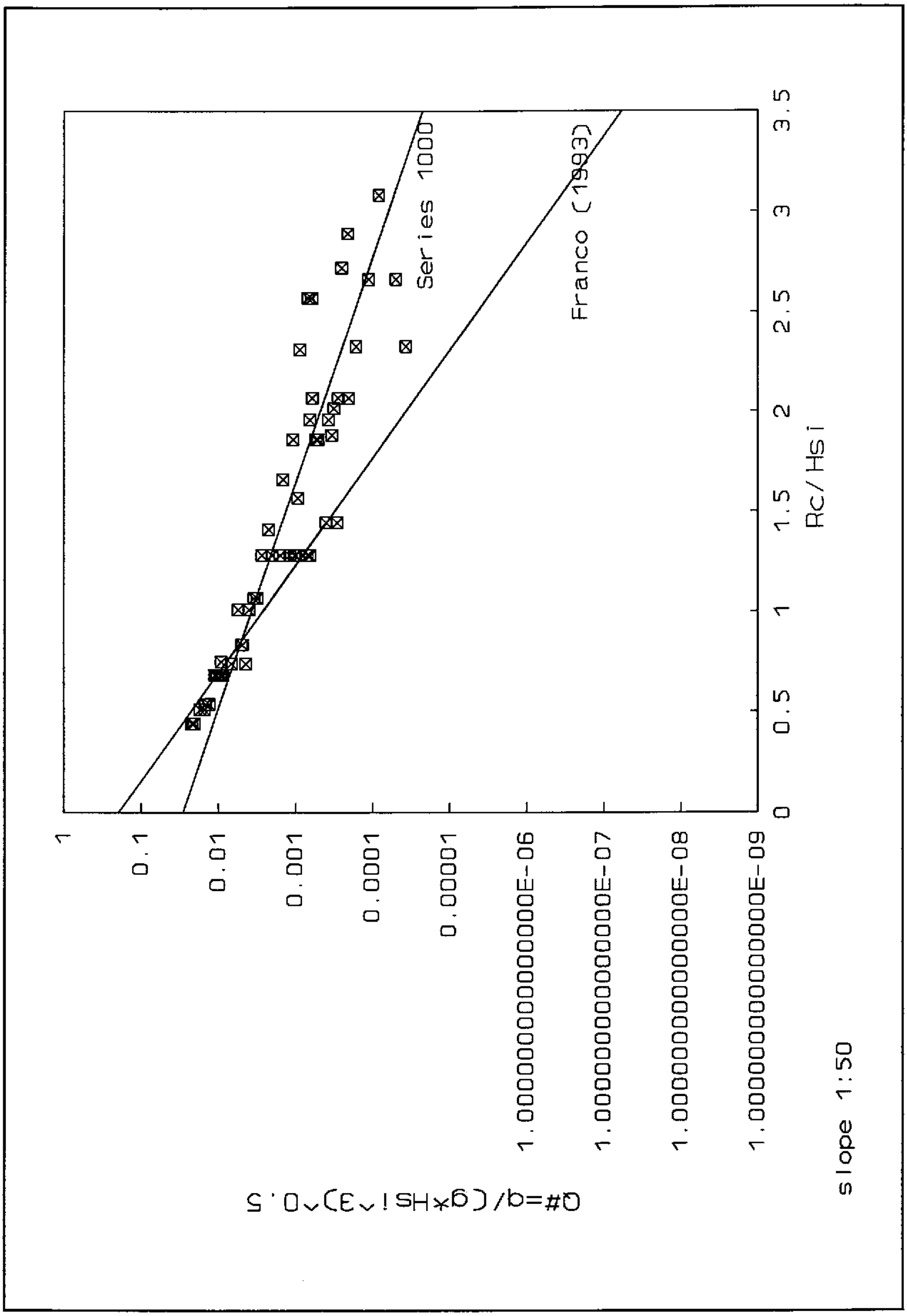

Figure 20 Simple vertical walls, Series 1000, Franco's equation

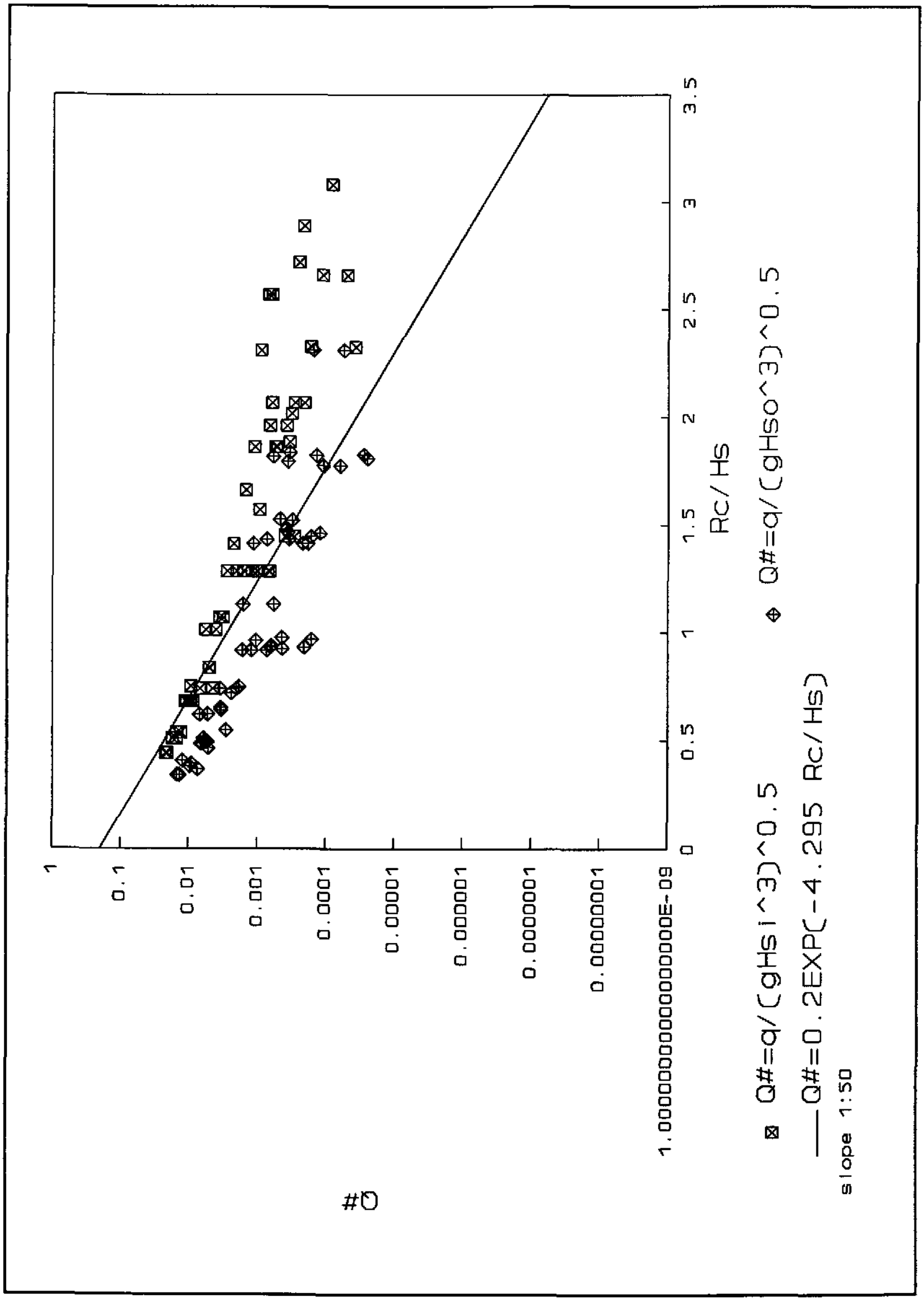

Figure 21 Franco's equation using offshore and inshore wave heights

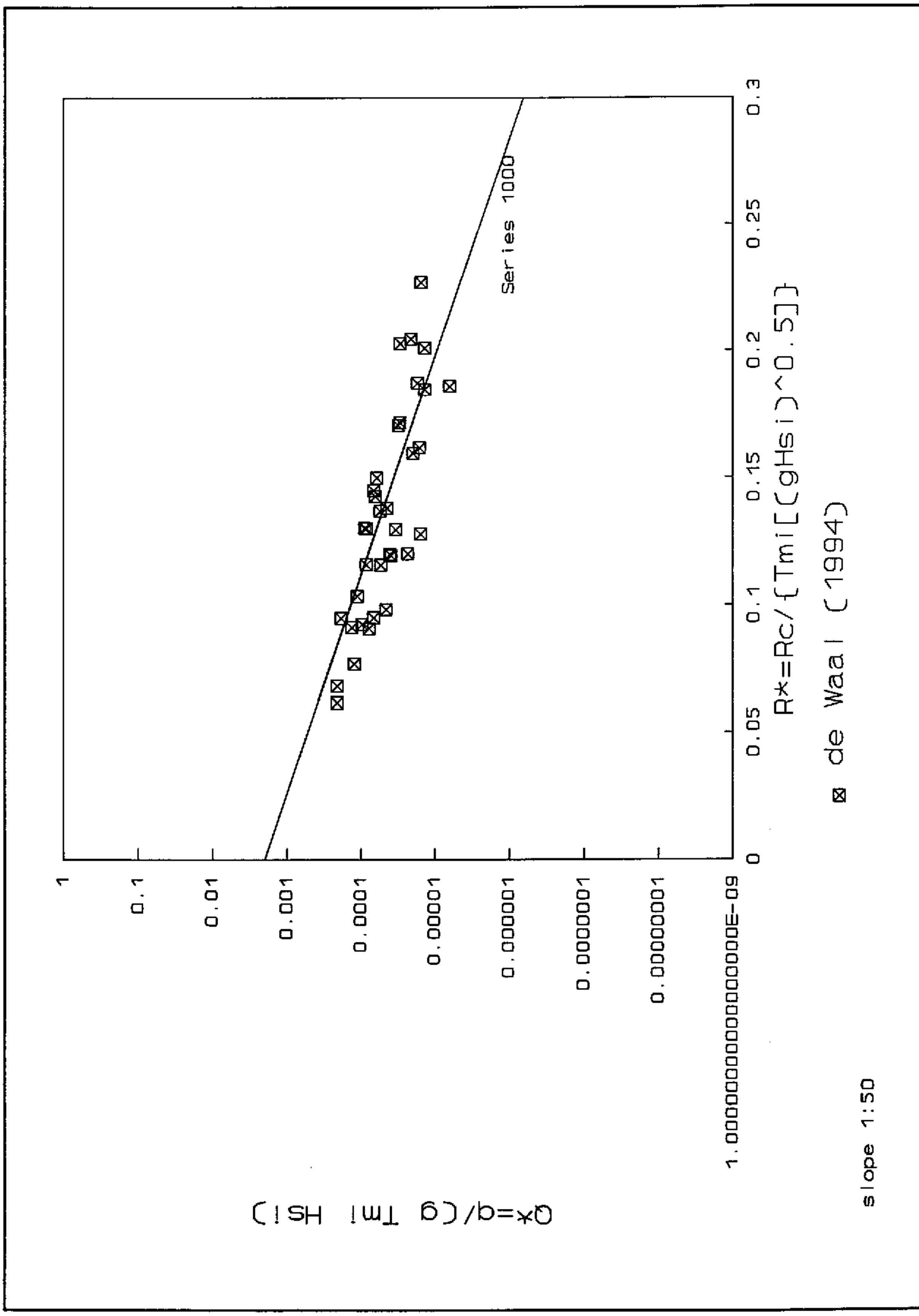

Figure 22 De Waal's data with Owen's equation, A=0.002 and B=26.76

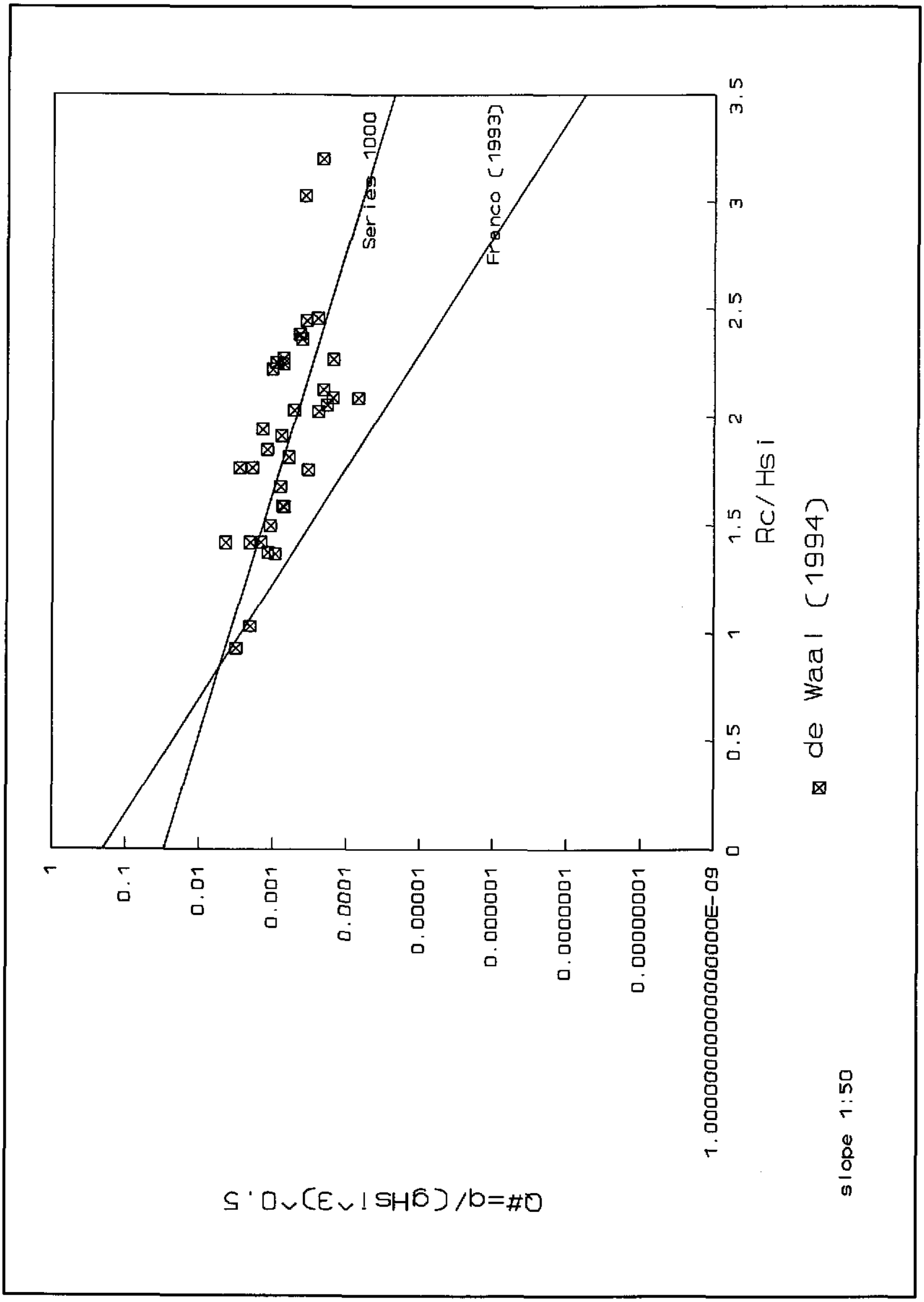

Figure 23 De Waal's data with Franco's equation, a=0.03 and b=-2.05

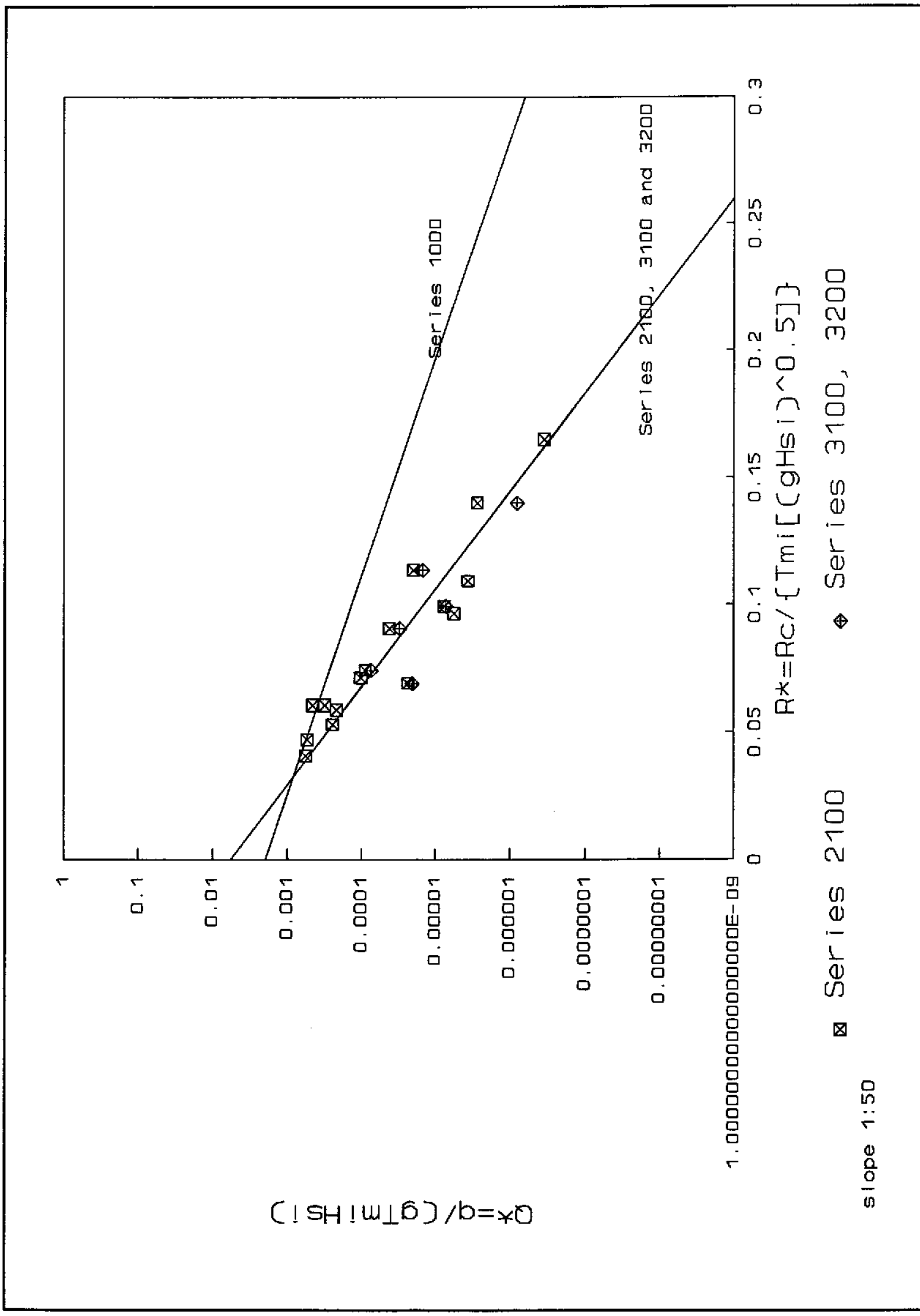

Figure 24 Single and double chamber wave screen structures, Series 2100, 3100 and 3200

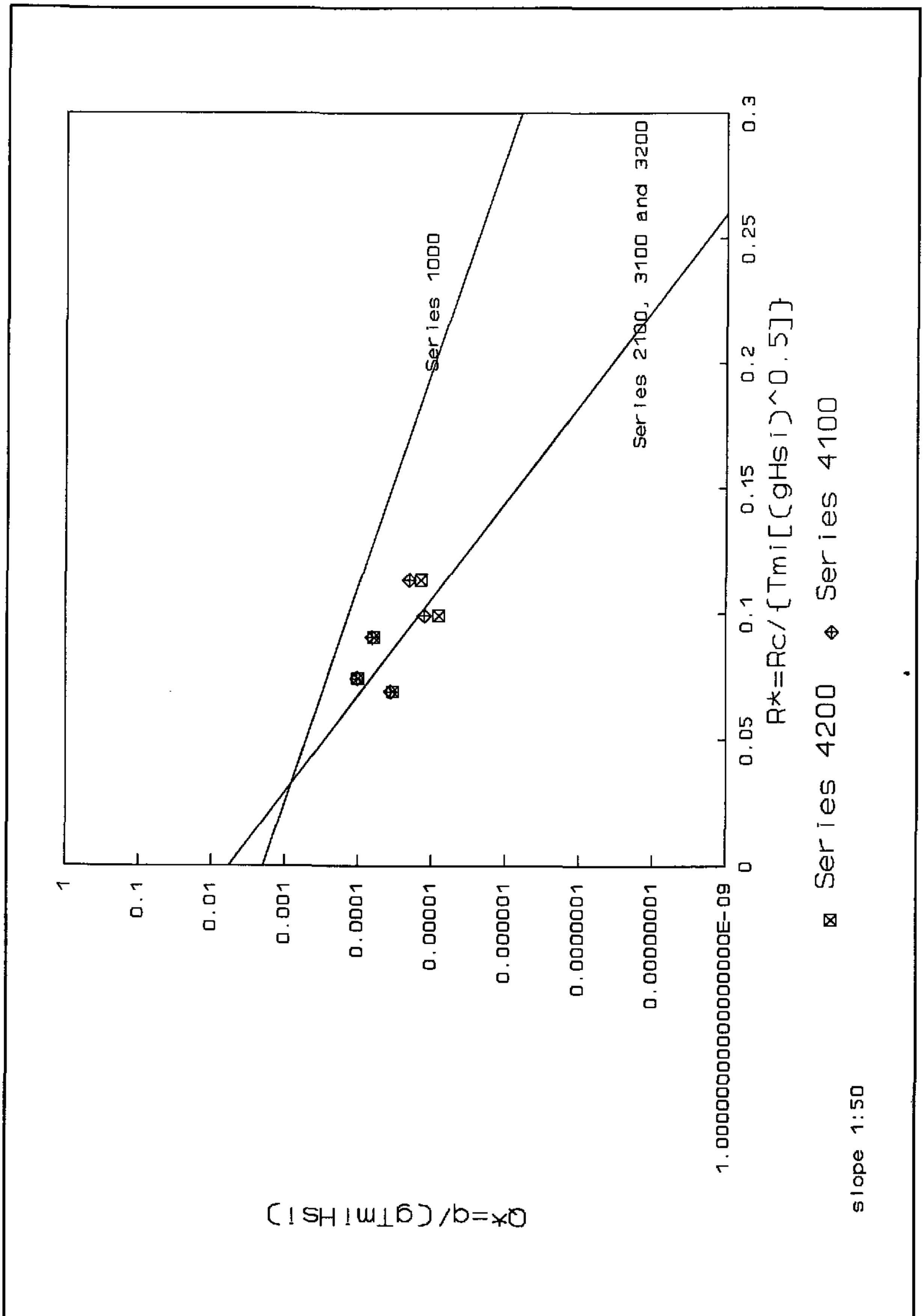

Figure 25 Wave screen structures, large holes, series 4200 and 4100

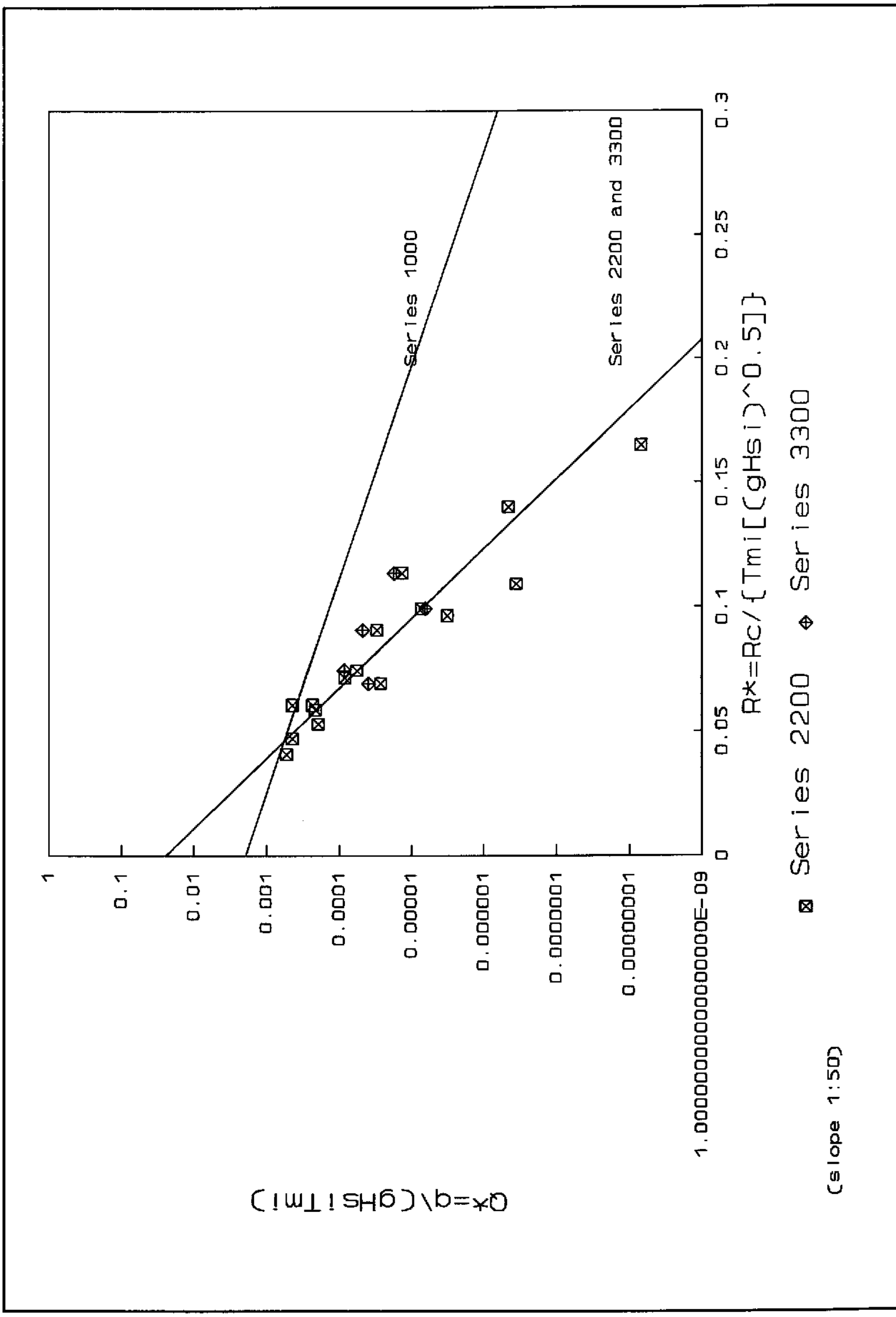

Figure 26 Wave screen structures, B_w=0.40m, Series 2200 and 3300

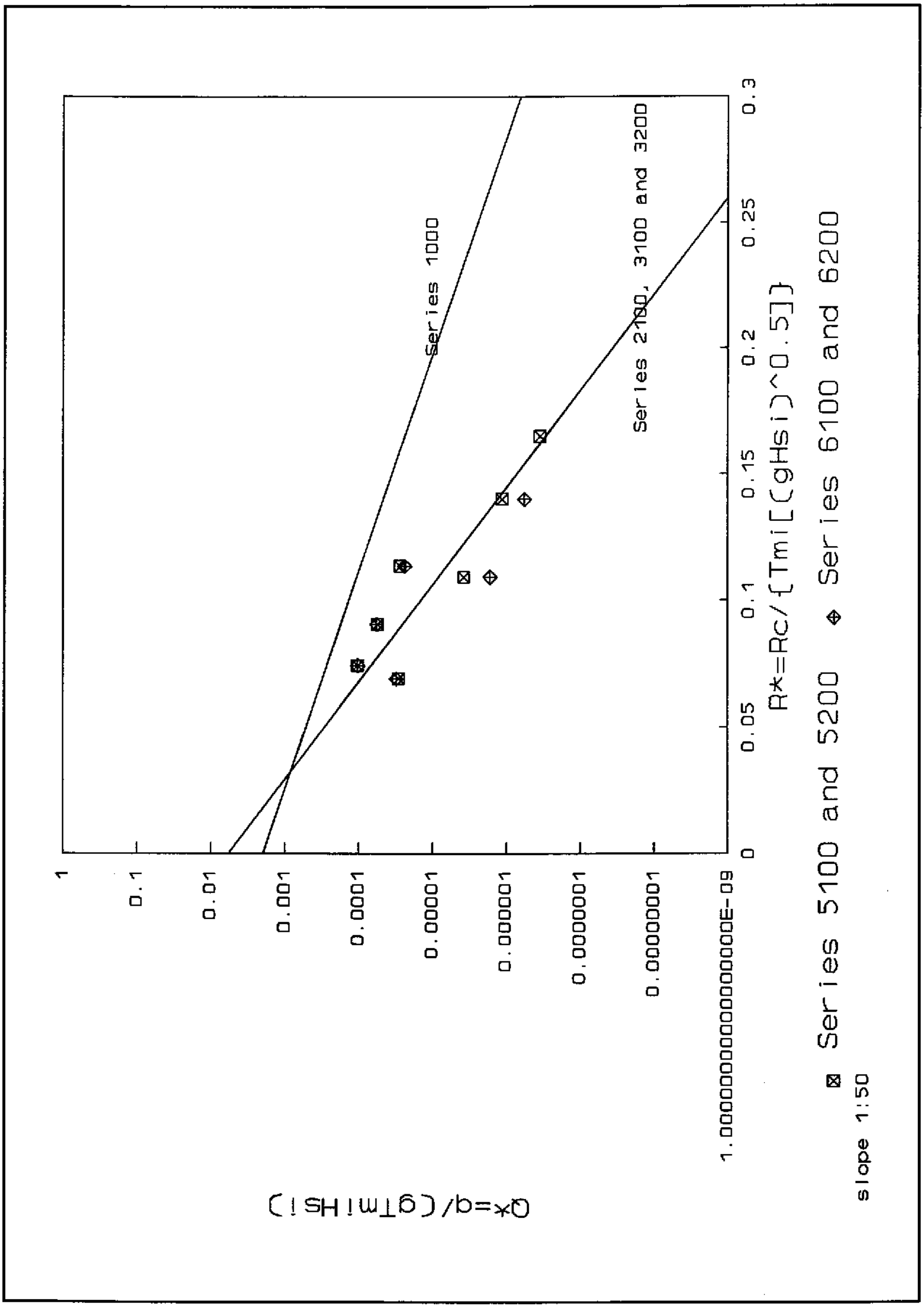

Figure 27 Caisson chambers with raised floors, Series 5000 and 6000

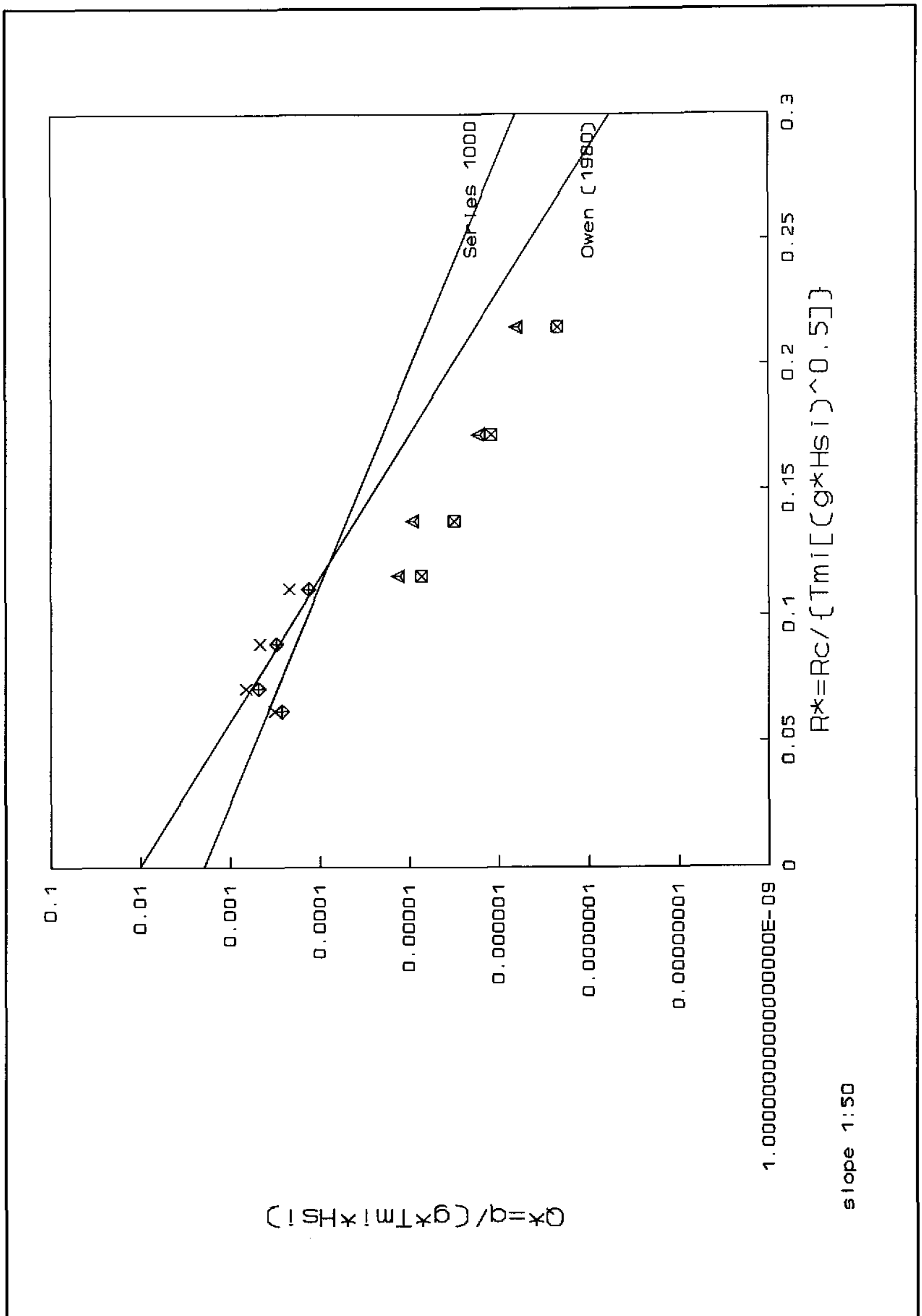

Figure 28 Overtopping of vertical wall with armoured slopes

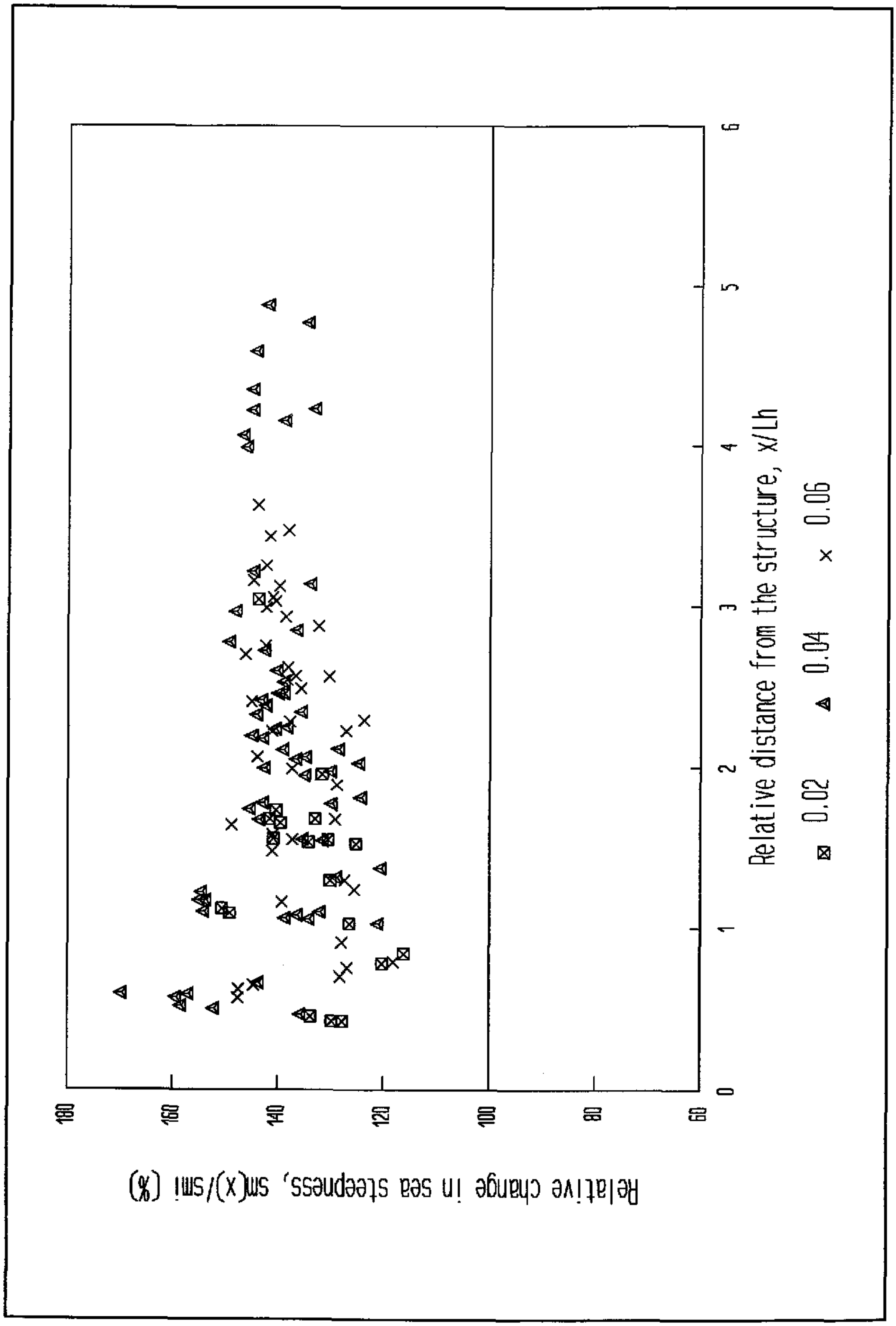

Figure 29 Water surface conditions - Vertical wall

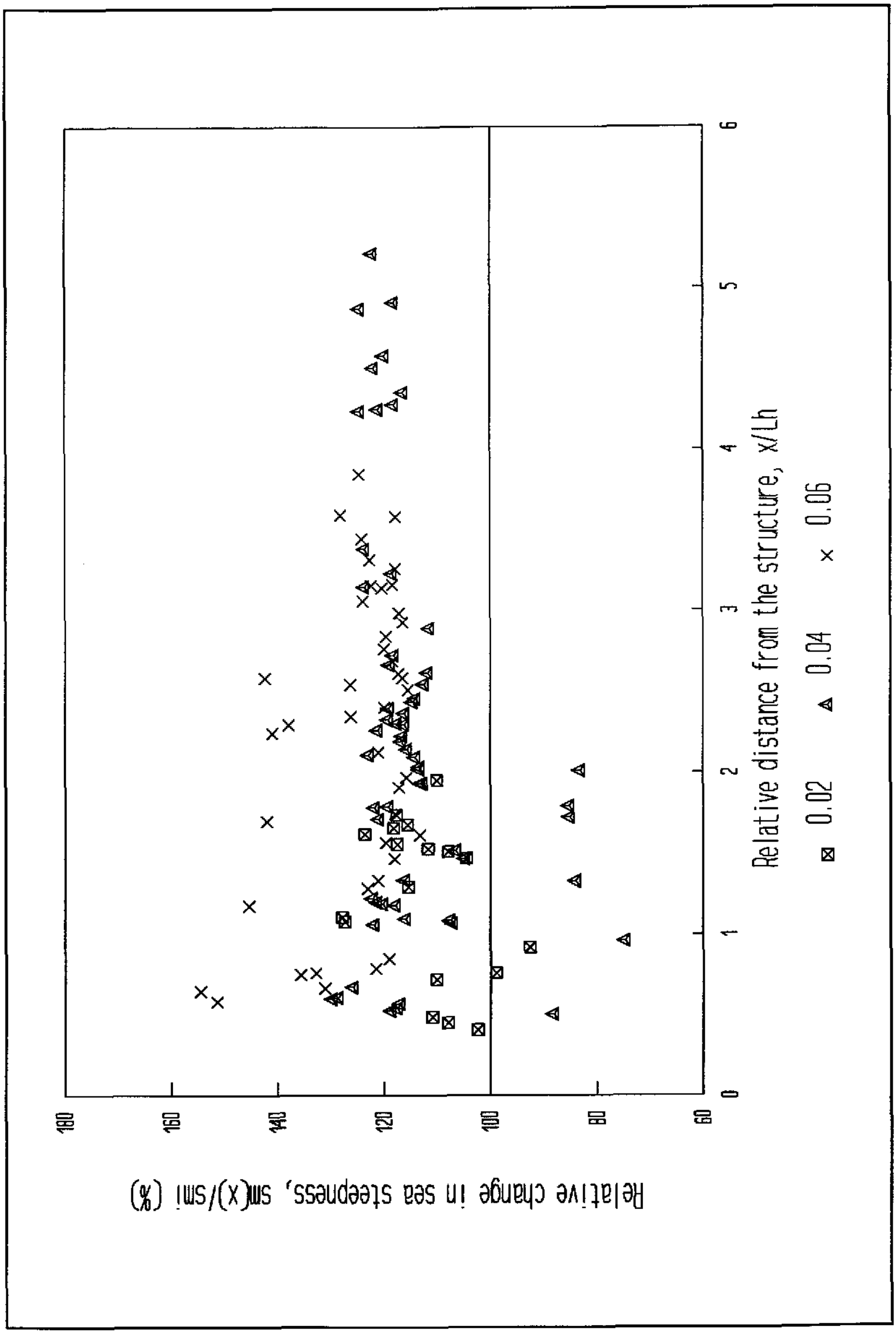

Figure 30 Water surface conditions - Single chamber wave screen

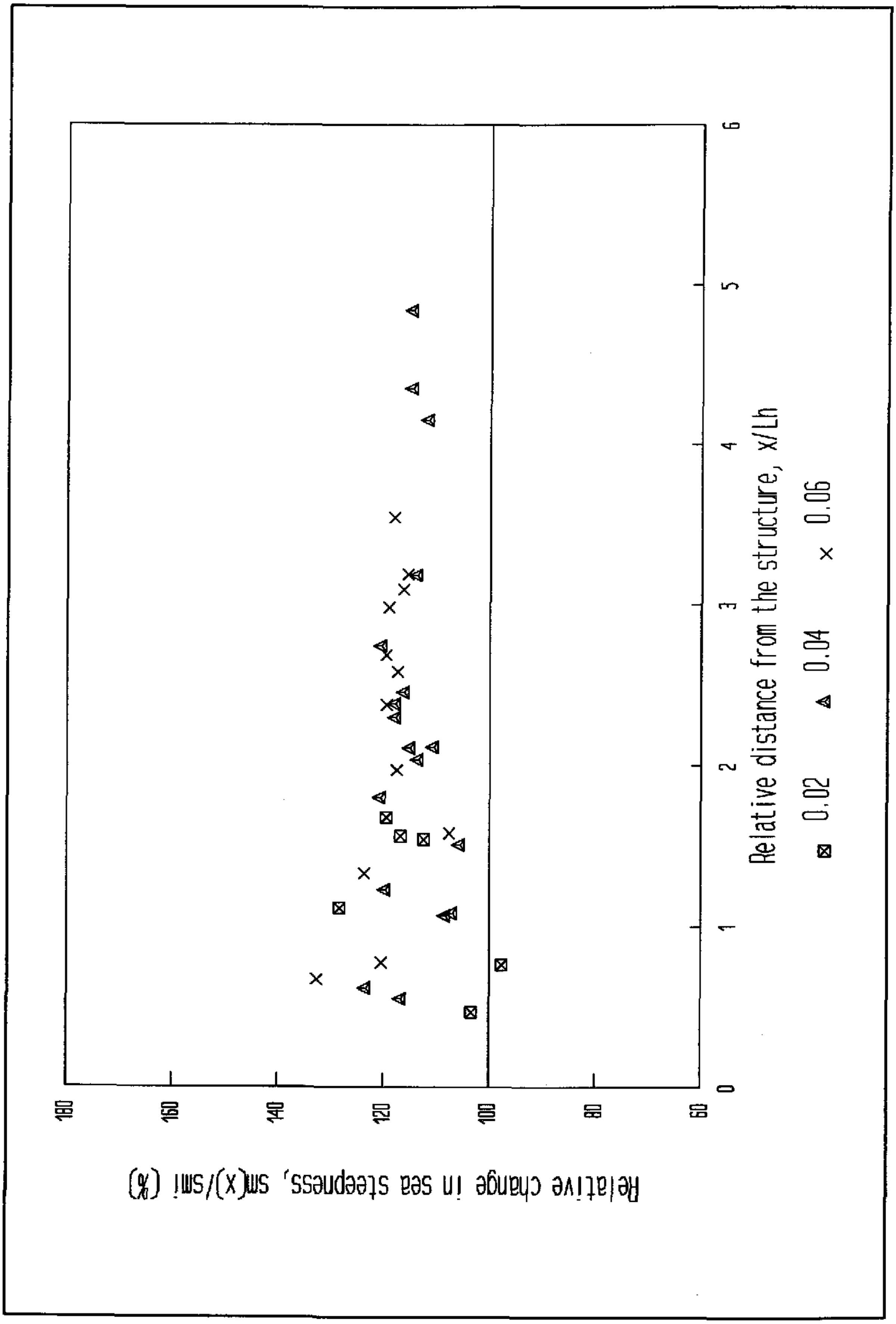

Figure 31 Water surface conditions - Double chamber wave screen

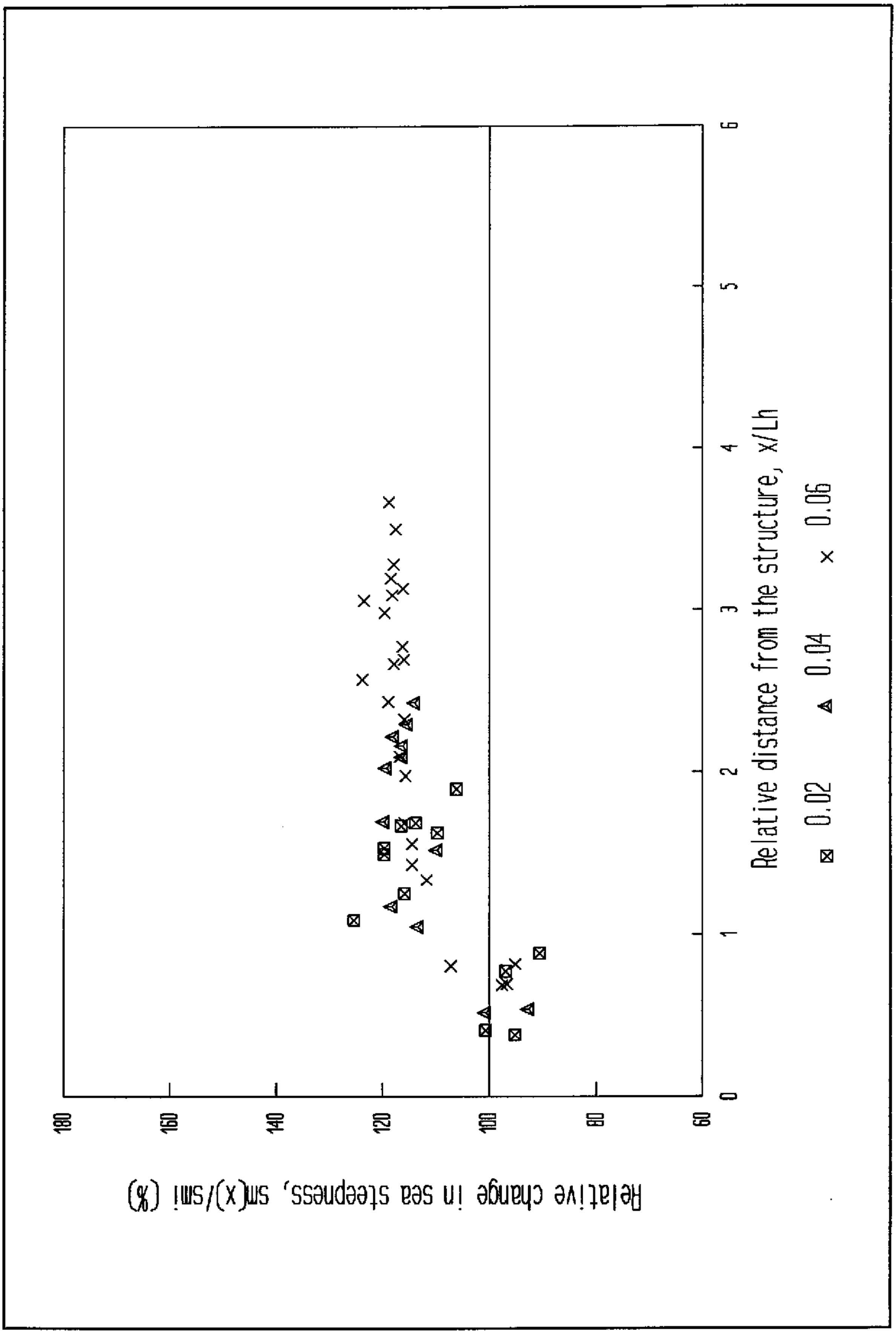

Figure 32 Water surface conditions - Rock armour slope

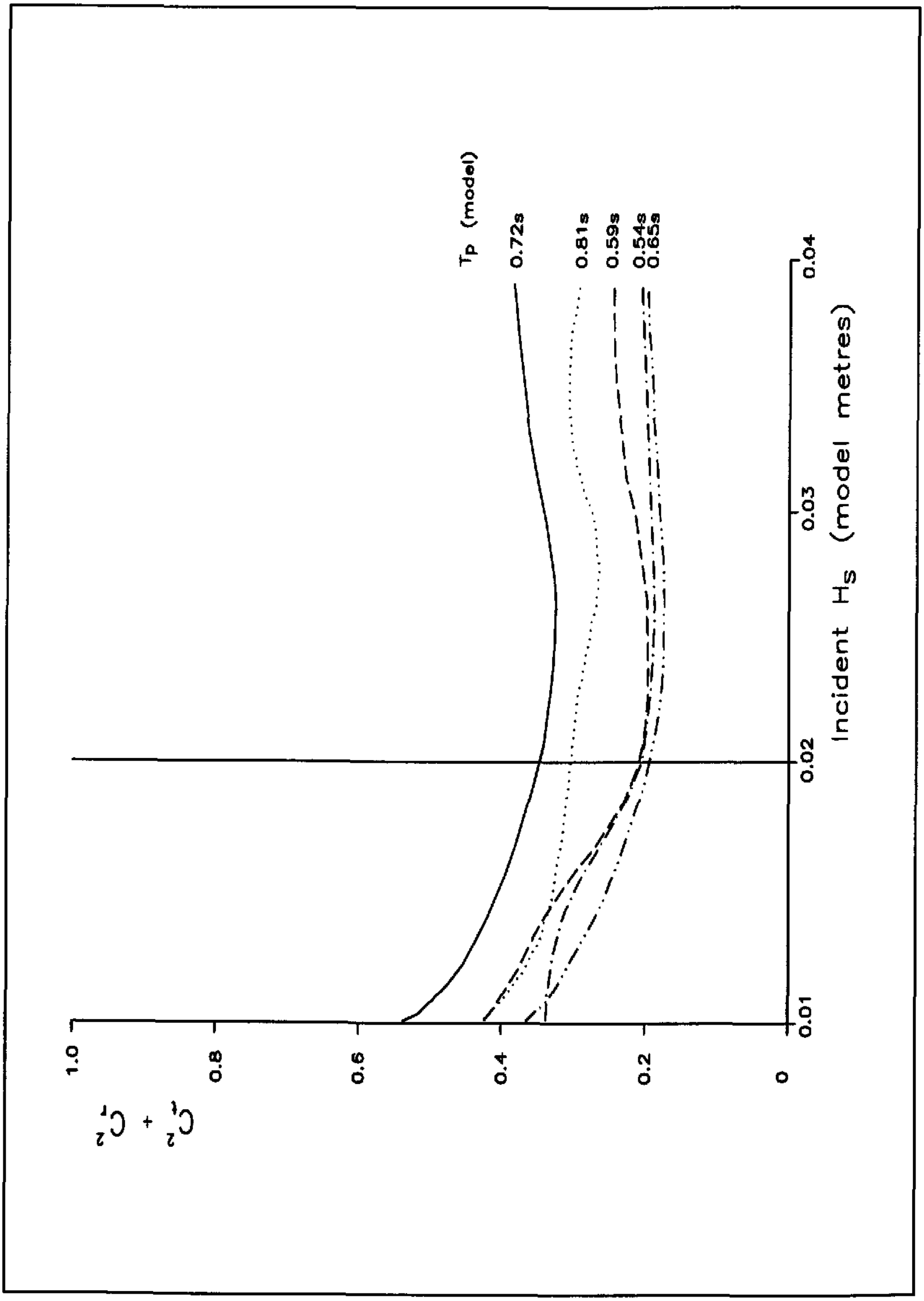

Figure 33 Analysis of scale effects for wave screens tested with small wave heights